



Biodegradable organic conductors for transient bioelectronics: materials design and degradation strategies

Myung-Kyun Choi^{1,#}, Jun-Hyeok Jeon^{1,#}, Yeon-Gyu Kim^{1,#}, Seung-Kyun Kang^{1,2,3,4,*}

Keywords:

Conjugated polymer, conductive composite paste, organic mixed ionic–electronic conductor, bioelectronics, biodegradability, softness

Citation:

Choi, M. K.; Jeon, J. H.; Kim, Y. G.; Kang, S. K. Biodegradable organic conductors for transient bioelectronics: materials design and degradation strategies. *Soft Sci.* 2026, 6, 51. <https://dx.doi.org/10.20517/ss.2026.71>

Received: 7 Apr 2026

First Decision: 24 Apr 2026

Revised: 29 Apr 2026

Accepted: 19 May 2026

Published: 17 Jun 2026

Academic Editor:

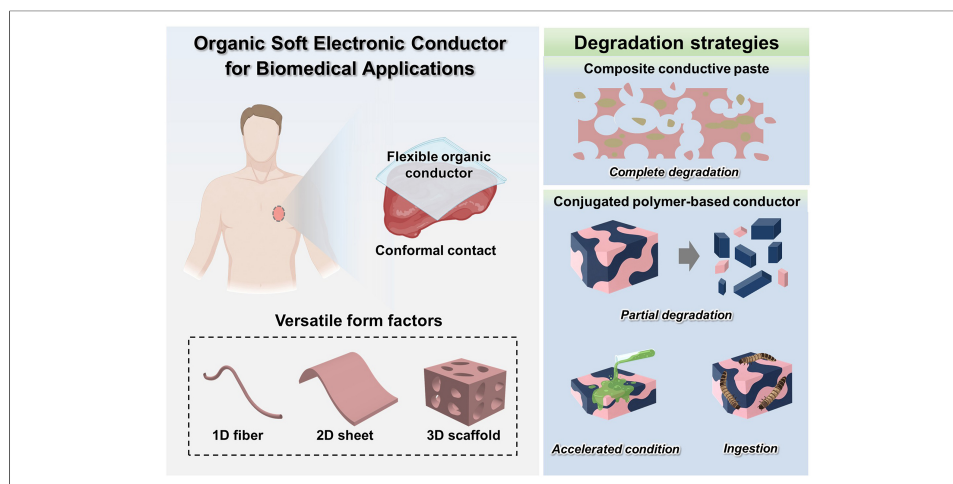
Raudel Avila

Copy Editor:

Pei-Yun Wang

Production Editor:

Pei-Yun Wang



Abstract

Biodegradable bioelectronic systems require materials that can mechanically integrate with soft tissues while minimizing long-term invasiveness. Conventional electronic materials, owing to their high stiffness, often cause mechanical mismatch with biological tissues, leading to chronic inflammation and tissue damage. To address these challenges, biodegradable conductive materials based on organic and polymeric systems have emerged as promising candidates for transient, biofriendly electronics. This review provides a comprehensive overview of recent advances in biodegradable conductive systems, including conductive polymers, conductive composite pastes, and organic mixed ionic–electronic conductors (OMIECs). The discussion covers material design strategies that simultaneously address electrical performance, mechanical compliance, and degradability in both partially and fully degradable systems. Particular attention is given to the relationships among degradation behavior, microstructure, and device stability, which play critical roles in determining functional lifetime. The scope further extends to key bioelectronic applications, including bioelectrical stimulation, drug delivery, sensing, and



¹Department of Materials Science and Engineering, Seoul National University, Seoul 08826, Republic of Korea.

²Interdisciplinary Program of Bioengineering, Seoul National University, Seoul 08826, Republic of Korea.

³Research Institute of Advanced Materials, Seoul National University, Seoul 08826, Republic of Korea.

⁴Soft Foundry Institute, Seoul National University, Seoul 08826, Republic of Korea.

#Authors contributed equally.

*Correspondence to: Prof. Seung-Kyun Kang, Department of Materials Science and Engineering, Seoul National University, Seoul 08826, Republic of Korea. E-mail: kskg7227@snu.ac.kr

neuromorphic systems, demonstrating the versatility of these materials across diverse platforms. Emphasis is placed on providing an integrated perspective for the design of next-generation transient bioelectronic systems based on biodegradable organic conductors.

INTRODUCTION

Bioelectronic systems increasingly require materials that minimize mechanical mismatch and long-term invasiveness in biological environments^[1,2]. Conventional electronic materials often exhibit elastic moduli in the range of tens to hundreds of GPa, which are substantially higher than those of biological tissues (kPa to MPa)^[3,4]. Such a mechanical mismatch can induce chronic inflammation, mechanical instability, and tissue damage during long-term implantation^[4-6]. Organic and polymer-based conductors offer a promising alternative due to their intrinsic mechanical softness and tissue-like mechanical properties. Their flexibility enables conformal contact with biological tissues, thereby reducing mechanical mismatch and minimizing inflammatory responses^[7]. These characteristics align with the broader concept of biofriendly electronic systems that aim to improve long-term biocompatibility and reduce device-induced tissue damage. Beyond mechanical compatibility, concerns regarding the long-term retention of materials in the body have further motivated the development of transient electronic systems^[8,9]. Biodegradable materials that degrade and resorb after functional operation eliminate the need for secondary surgical removal and reduce long-term burden of implanted devices. In this context, transient organic-based conductors provide a compelling material platform that combines mechanical softness, biocompatibility, and controlled biodegradability, thereby enabling minimally invasive, biofriendly electronic systems [Figure 1].

Organic electronic materials, typically based on polymeric conductors, inherently offer mechanical compliance, low-temperature processability, and high compatibility with diverse form factors, enabling conformal interfaces with soft biological tissues^[7,10]. These properties facilitate minimally invasive integration and stable operation under mechanical deformation^[11,12]. At the same time, transient functionality enables controlled degradation after use, thereby reducing long-term material retention and eliminating the need for surgical removal. This capability is particularly advantageous for temporary therapeutic, diagnostic, and monitoring applications, where device operation is required only for a limited period. In this regard, organic transient electronic materials provide a unified strategy for the development of biofriendly electronic systems, supporting both short-term functionality and safe end-of-life behavior.

Early studies on polymer-based biodegradable conductors focused primarily on conductive polymers, in which charge transport occurs via delocalized π -electrons along conjugated backbones^[13-15]. From the perspective of degradation behavior, these materials can be broadly classified into partially degradable and fully degradable systems, as illustrated in Figure 2. For partially degradable conjugated polymer systems, representative strategies include blending with biodegradable polymers^[16-19], copolymerization with degradable segments^[20,21], and grafting conjugated chains onto biodegradable backbones^[22-28]. In these cases, degradation mainly occurs in the biodegradable components, while the conjugated backbone remains relatively persistent, making complete degradation difficult. In contrast, fully degradable conjugated polymer systems aim to eliminate residual structures by cleaving the conjugated backbone through mechanisms such as ingestion-triggered degradation, enzymatic reactions, and acid-catalyzed hydrolysis. For example, metabolic degradation by superworms^[29], macrophage-mediated phagocytosis induced by conjugated oligomers^[30], and the introduction of acid-cleavable linkages^[31] have been reported. However, these approaches have limitations, including insufficient degradation under physiological conditions and reduced electrical conductivity due to shorter conjugated chain lengths introduced to enhance degradability^[18].

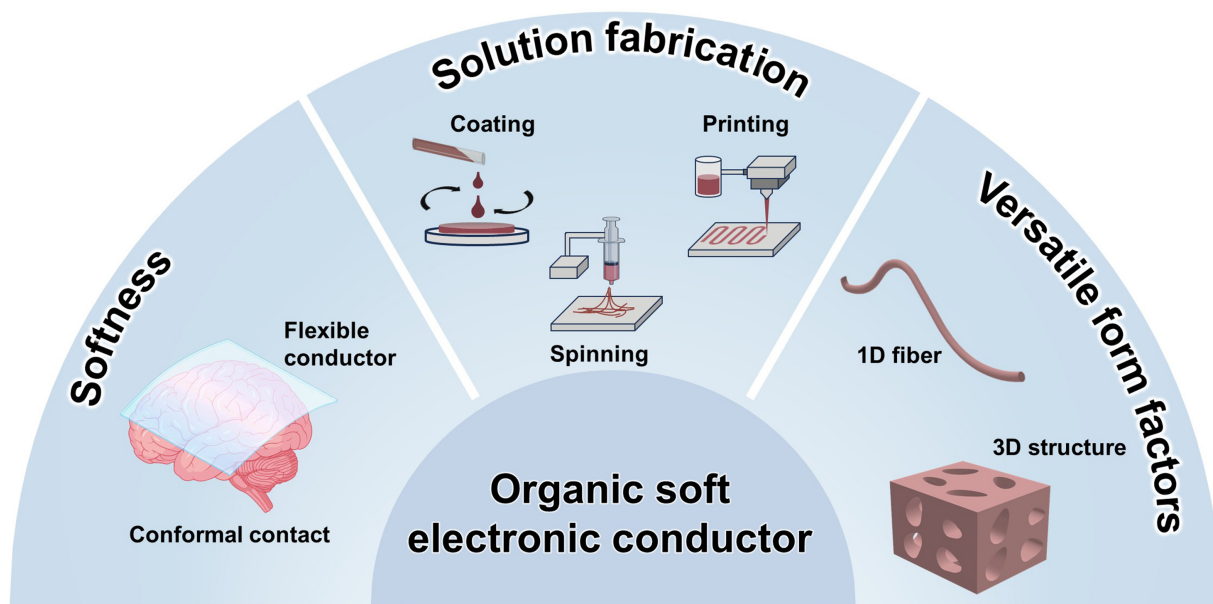


Figure 1. Overview of solution-processed organic soft conductors. Created in BioRender [Bio-Interfaced Electronics, L. (2026) <https://BioRender.com/b1rd9op>].

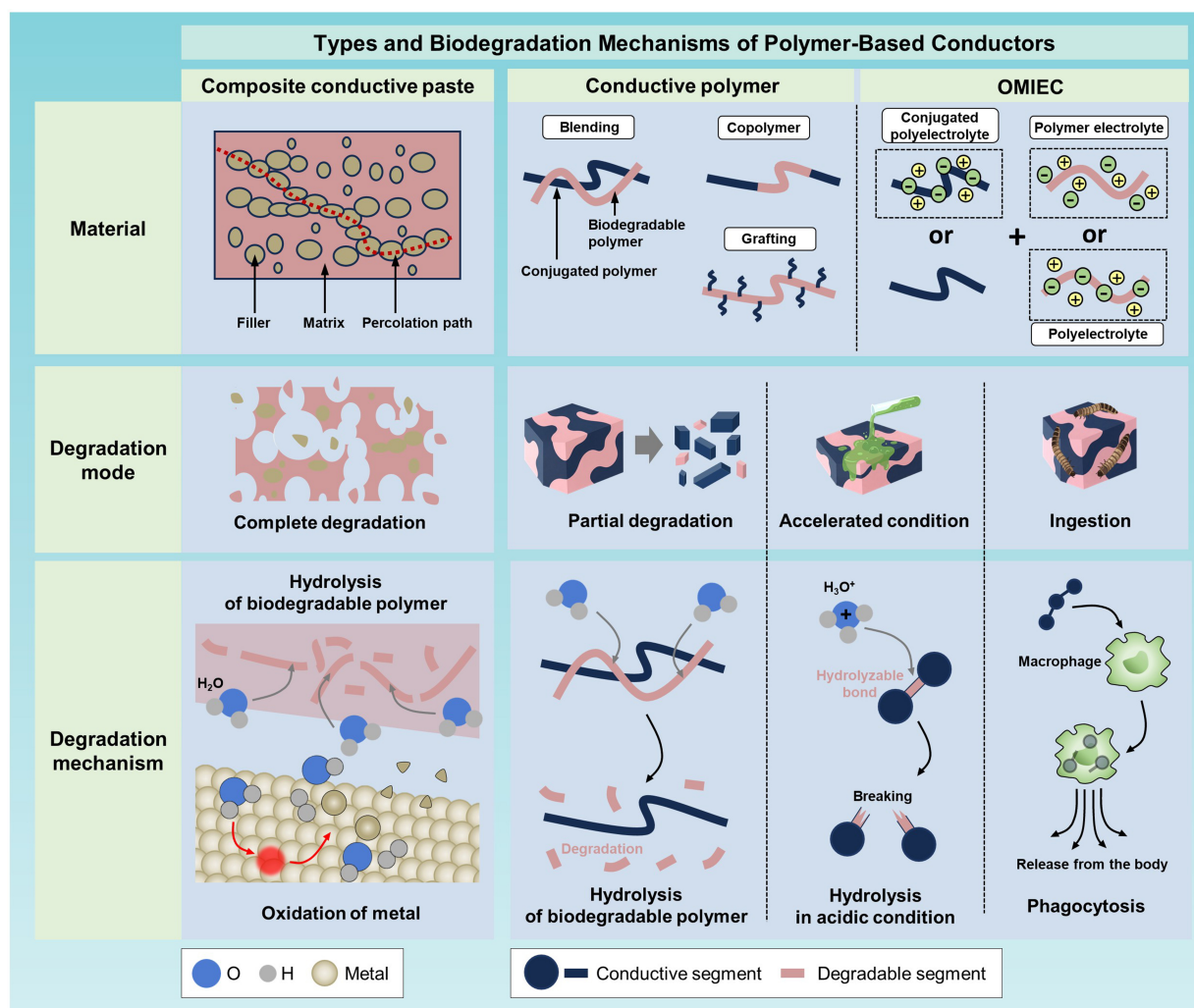


Figure 2. Classification and biodegradation mechanisms of polymer-based conductors, including conductive composite pastes, biodegradable conductive polymers, and OMIECs. Created in BioRender [Bio-Interfaced Electronics, L. (2026) <https://BioRender.com/128cgy>]. OMIECs: Organic mixed ionic–electronic conductors.

These limitations highlight that introducing biodegradability into conductive polymers inevitably disrupts charge-transport pathways and π -conjugation, leading to a trade-off between electrical performance and degradability. Therefore, rational material design should focus on preserving continuous conduction networks and maintaining conductive segment length. In addition, degradable moieties should be selectively engineered to ensure compatibility with physiological degradation conditions. To address these limitations, conductive composite pastes have been proposed as an alternative material platform. As illustrated in [Figure 2](#), these systems consist of biodegradable conductive inorganic fillers dispersed within a biodegradable polymer matrix, where percolation networks formed by interparticle contacts establish continuous conductive pathways^[32-34]. The degradation mechanism involves corrosion or dissolution of conductive fillers together with hydrolysis of the polymer matrix, leading to the breakdown of the percolation network and eventual loss of conductivity. Nevertheless, this strategy enables high electrical conductivity while simultaneously achieving overall biodegradability^[35]. However, introducing biodegradability into conductive composite pastes often leads to premature degradation of percolation networks in aqueous environments. This results in a rapid loss of electrical conductivity that is decoupled from bulk material degradation. Therefore, rational design should focus on stabilizing interparticle contacts and preserving network integrity through interface engineering, controlled filler dispersion, and protective encapsulation to ensure reliable device operation within the intended functional lifetime.

Recent advances have increasingly focused on expanding functionalities, including logic operations, active device integration, and compatibility with biological ionic signals, driving the rapid development of organic mixed ionic–electronic conductors (OMIECs)^[36]. OMIECs combine electronic conduction in conjugated polymers with ionic conduction, enabling the simultaneous transport of ions and electrons^[36]. This coupled ion–electron transport allows dynamic modulation of conductivity in electrolyte environments, high signal amplification at low operating voltages, and direct interaction with biological ionic signals, thereby making OMIECs particularly suitable for neural interfacing and biosensing applications^[36]. From the perspective of biodegradability, OMIECs can be classified into partially and fully degradable systems. Partially degradable OMIECs are typically designed by incorporating biodegradable ionic conductors, resulting in the selective hydrolysis of the ionic conducting components while the conjugated backbone remains intact^[37-44]. Furthermore, strategies to achieve fully biodegradable systems are being explored, including the introduction of hydrolytically cleavable segments into the conjugated backbone and the utilization of enzymatic or metabolic degradation pathways^[29,45,46]. Although complete biodegradation to monomeric species is often pursued, such degradation typically requires accelerated acidic conditions^[45,46], and the potential toxicity of π -conjugated monomers must also be considered. Moreover, because biodegradability and material reliability are often in a trade-off relationship, the development of biodegradable OMIECs requires not only degradable backbone chemistry but also careful structural design to balance stability, degradation behavior, and biocompatibility.

Despite these advances, existing review articles have largely focused on individual material systems or specific application domains, lacking a unified perspective across different classes of organic conductors. In particular, the fundamental relationships among electrical performance, mechanical compliance, and biodegradability have not been systematically addressed, and emerging materials such as OMIECs remain underexplored in this context. Therefore, a comprehensive framework that integrates intrinsically conducting polymers, conductive composites, and OMIECs is still needed to guide the rational design of biodegradable organic conductors. Here, we first discuss conductive polymers, focusing on molecular design strategies that introduce hydrolyzable functional groups into conjugated backbones or side chains, and examine how these modifications govern degradation pathways and correlate with charge transport properties. We then examine conductive polymer composites, in which the interactions between biodegradable matrices and conductive fillers, along with structural disintegration behavior, determine

Table 1. Characteristic properties of conductive polymers

Materials	Conductivity (S/cm)	Modulus (MPa)
PPy	2-100 ^[49]	-55 ^[50]
PANI	0.01-1 ^[49]	-
Polythiophene	1-1,000 ^[49]	-
PDA	-0.001 ^[51]	12,000 ^[51,52]
Melanin	-0.001 ^[53]	-

PPy: Polypyrrole; PANI: polyaniline; PDA: polydopamine.

Table 2. Advantages, limitations, and applications of biodegradable conductive polymers according to synthesis strategies

	Advantage	Limitation	Applicability
Blending (<i>in-situ</i> polymerization)	Tunable conductivity Simple synthesis	Phase separation Percolation threshold	Physical and chemical sensor
Main-chain copolymer	Various degradation strategies Intrinsic system	Limited charge transport efficiency Synthetic complexity Limited design flexibility	Biomedical application
Grafting copolymer	Balanced properties tunability	Partial degradation Complex synthesis	Physical sensor Biomedical application

mechanical stability and the retention of conductive pathways during degradation. Finally, we discuss OMIEC systems, highlighting how ionic–electronic coupled transport and the degradation behavior of both ionic conductors and conjugated polymers influence electrochemical performance and operational stability. We further discuss how the intrinsic material characteristics of these conductors are translated into a wide range of device components, from passive elements such as interconnects and electrodes to active devices including transistors and neuromorphic systems, as well as how they are ultimately utilized in biointerface systems.

BIODEGRADABLE CONDUCTIVE POLYMERS FOR SOFT ELECTRONICS

Biodegradable conductive polymers balance electrical conductivity with mechanical compliance and controlled degradation, presenting a central materials challenge in transient soft electronics. Conductive polymers are inherently attractive due to their electronic functionality, biocompatibility, and chemical tunability^[47]. High conductivity arises from extended π -conjugation, strong intermolecular interactions, and structural ordering. However, these features often lead to increased stiffness and brittleness^[48] [Table 1]. In contrast, improving mechanical flexibility and biodegradability typically requires the introduction of flexible segments or labile linkages, which can disrupt conjugation pathways and reduce electrical performance^[47]. This trade-off constrains their implementation in biointegrated and transient systems that require soft mechanical properties and predictable degradation profiles^[39].

To overcome these limitations, various material design strategies have been developed to introduce degradability without compromising the integrity of the charge-transport network [Table 2]. These strategies can be broadly categorized into two types based on their degradation behavior^[47]. The first is a partially degradable system, in which the conductive polymer backbone remains intact even after the surrounding biodegradable matrix has decomposed. The second is a fully degradable strategy designed to break down the entire conductive system into environmentally or biologically benign substances. This classification reflects the fundamental trade-off between electrical performance and degradability and provides a useful framework for understanding current material design approaches.

Table 3. Degradation kinetics of individual biodegradable polymer matrices

Materials	Dissolution conditions			Degradation rate [wt.% day ⁻¹]	
	Type	pH	Temperature [°C]		
Natural polymer	Starch	Natural seawater	-	-	2 ^[55]
	CS	Soil	-	-	15–25 ^[56]
	Chitin	Lysozyme (in PBS)	7.4	37	40–70 ^[57]
	Collagen	PBS	7.4	20	0.16–1.44 ^[58]
	PHB	Lipase (in PBS)	7.4	37	0.06 ^[59]
	CNF	Soil	5.7, 8.1	-	2.0–2.3 ^[60]
	PGS	PBS	7.4	37	0.36 ^[54]
Synthetic polymer	PGA	DI water	-	40–50	0.3–1.6 ^[61]
	PEA	Proteinase K in Tris-HCl buffer	7.4	37	7.2 ^[24]
	Polyphosphazene	PBS, borate buffer	7.4, 7	37	0.08–1.84 ^[62]

CS: Chitosan; PBS: phosphate-buffered saline; PHB: poly(3-hydroxybutyrate); CNF: cellulose nanofiber; PGS: poly(glycerol sebacate); PGA: poly(glycolic acid); DI: deionized; PEA: poly(ester amide).

Partially degradable conductive polymer systems

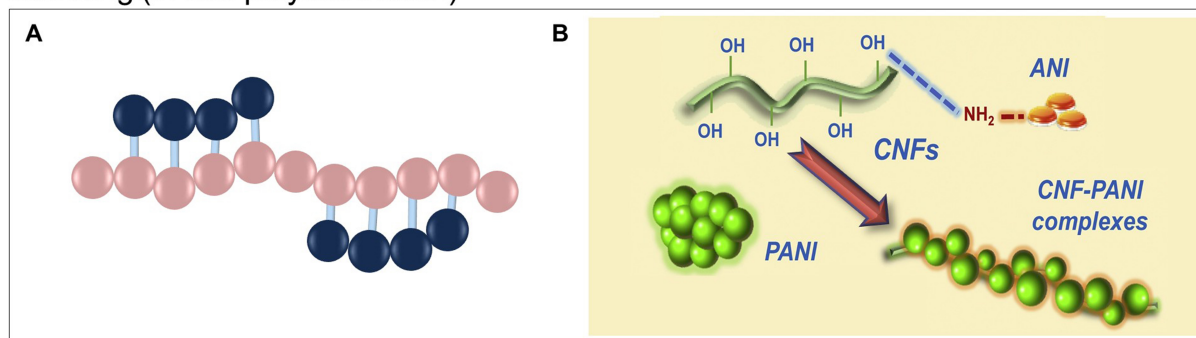
In this section, we first examine the partially degradable systems predominantly used in current implementations, followed by a review of emerging strategies toward fully degradable conducting polymers. Furthermore, we discuss the applications of each system in electronics and the remaining challenges in the field. Initial strategies for partially degradable systems focused on blending conductive polymers with biodegradable matrices to impart mechanical softness and biological compatibility^[15] [Table 3]. Natural polymers such as chitosan (CS) and its derivatives have been widely used for this purpose due to their intrinsic biocompatibility and flexibility^[22,63–66]. However, the inherent incompatibility between hydrophobic conductive polymers and hydrophilic biodegradable matrices often leads to phase separation, weak interfacial adhesion, and disrupted charge-transport pathways^[67]. As a result, high loading fractions of conductive components are typically required to establish continuous conductive pathways, which suppresses degradation and compromises mechanical integrity^[68,69]. For example, polypyrrole (PPy) blended with biodegradable matrices such as poly(glycerol sebacate) (PGS)/collagen requires high conductive content to achieve measurable conductivity, highlighting the trade-off between electrical performance and degradability in physically blended systems^[54].

In situ polymerization within biodegradable templates provides a more effective route to improve interfacial compatibility and maintain conductive pathways^[16,18,70] [Figure 3A]. In this approach, conductive monomers such as aniline^[74], pyrrole^[19], and 3,4-ethylenedioxythiophene (EDOT)^[39] are polymerized directly within a polymer matrix, forming interpenetrating networks with improved dispersion and structural integrity^[75]. This strategy enables the simultaneous enhancement of mechanical and electrical properties.

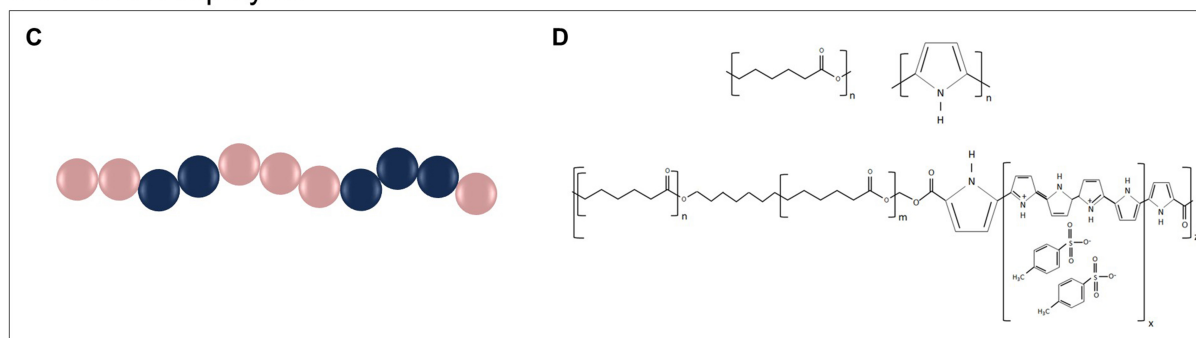
Figure 3B demonstrates the synthesis of nanocellulose-templated polyaniline (PANI), which produces elastomeric composites with a mechanical strength of ~10 MPa, stretchability exceeding 500%, and conductivity in the range of ~10⁻³ S·cm⁻¹. These results demonstrate that bio-templated architectures can mitigate phase separation while preserving conductive pathways, although precise control over the microstructure remains essential for reproducible performance^[71].

Block copolymerization offers a more controlled strategy by integrating conductive and biodegradable segments within a single macromolecular architecture^[76] [Figure 3C]. Synthetic biodegradable polymers such as polycaprolactone (PCL)^[21] and polylactic acid (PLA)^[77] are commonly employed to ensure structural

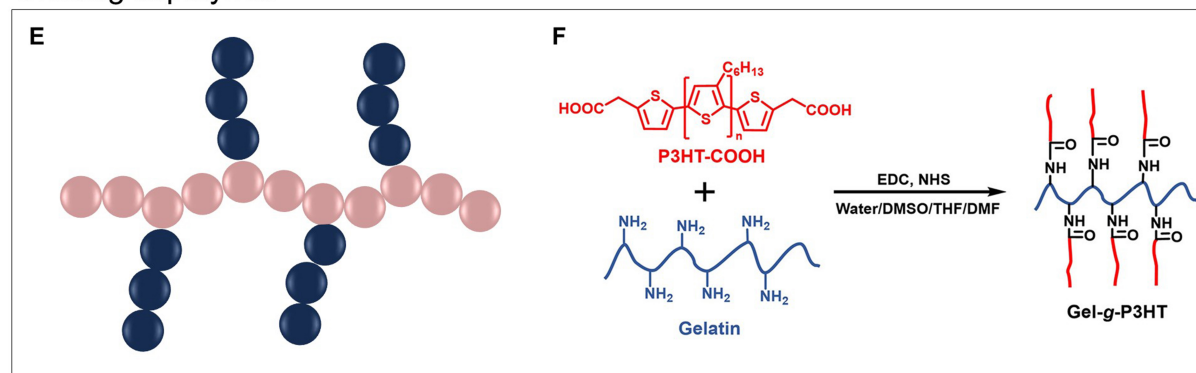
Blending (in-situ polymerization)



Main-chain copolymer



Grafting copolymer



● = Degradable unit ● = Conductive unit — = Intermolecular interaction

Figure 3. Various synthesis strategies for tailoring the properties of partially biodegradable conductive polymers. (A) Blending strategy involving the *in situ* polymerization of conductive polymers within biodegradable polymer matrices, featuring biodegradable backbones and *in situ*-formed conductive segments through intermolecular interactions; (B) Schematic illustration of the formation of CNF-PANI polymer blends via *in situ* polymerization. Reprinted with permission from Ref. [771]. Copyright 2019, Elsevier; (C) Main-chain copolymer strategy, in which degradable and conductive segments are incorporated into a single backbone in a repeating manner; (D) Chemical structures of the biodegradable PCL segment, the conductive PPy polymer, and the resulting conductive PPy-*b*-PCL block copolymer. Reproduced with permission from Ref. [721] under the CC BY license; (E) Grafting copolymer strategy for attaching conductive segments to a biodegradable backbone; (F) Schematic illustration of the synthesis of Gel-g-P3HT and grafting of P3HT-COOH onto gelatin via an EDC/NHS coupling reaction. Reprinted with permission from Ref. [731]. Copyright 2024, American Chemical Society. CNF: Cellulose nanofiber; PANI: polyaniline; PCL: polycaprolactone; PPy: polypyrrole; Gel-g-P3HT: gelatin-grafted poly(3-hexylthiophene-2,5-diyl); EDC: N-(3-dimethylaminopropyl)-N'-ethylcarbodiimide; NHS: N-hydroxysuccinimide; ANI: aniline.

uniformity and reduce side reactions. Figure 3D illustrates that block copolymers such as PPy-*b*-PCL significantly improve mechanical compliance while maintaining electrical conductivity on the order of $10^{-2} \text{ S}\cdot\text{cm}^{-1}$, with mechanical properties approaching those of soft biological tissues in the MPa range. These systems exhibit partial degradation, with mass loss reaching $\sim 50\%$ over several weeks under accelerated

conditions^[72]. Nonetheless, phase segregation within polymer domains can still limit charge-transport efficiency and long-term stability, indicating that the balance between electronic connectivity and degradability remains unresolved^[78].

Graft copolymer approaches provide an alternative approach in which conductive side chains are attached to a biodegradable backbone, enabling greater molecular design versatility^[79] [Figure 3E]. For example, poly(3,4-ethylenedioxythiophene) (PEDOT) grafted with poly-D,L-lactic acid (PDLLA) retains electrical conductivity for several weeks during degradation, demonstrating improved stability relative to physically blended systems^[80]. However, increasing the fraction of biodegradable chains disrupts interchain π - π stacking, leading to a substantial reduction in conductivity, often by several orders of magnitude. Figure 3F shows the properties of gelatin-grafted poly(3-hexylthiophene-2,5-diyl) (Gel-g-P3HT), where P3HT segments are integrated onto a biodegradable gelatin backbone. In this architecture, structural ordering enables partial recovery of conductivity ($\sim 10^{-7}$ S·cm⁻¹), although the overall electrical performance remains limited compared to pristine conductive polymers^[73].

Despite these advances, most current strategies yield only partially biodegradable systems, as the conductive polymer backbone often persists after degradation of the surrounding matrix. This limitation restricts their applicability in fully transient electronic systems and underscores the need for intrinsically degradable conjugated polymers that retain electrical functionality while undergoing complete breakdown^[81]. Future progress will require improved control over molecular design, microstructure, and phase behavior, together with strategies that balance conductivity, mechanical compliance, and degradation kinetics. Achieving this balance remains a central challenge in the development of biodegradable conductive polymers for transient soft electronics.

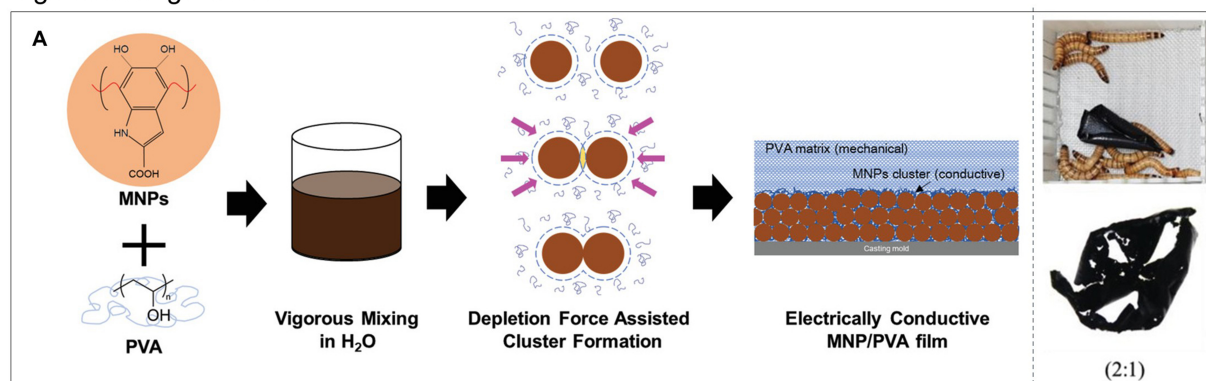
Fully degradable strategies of conductive polymers

In contrast to partially degradable systems, fully degradable conductive polymers are designed to enable complete decomposition of the conductive network into environmentally or biologically benign products. Achieving this capability requires molecular design strategies that preserve charge transport while allowing controlled degradation under physiological or environmental conditions^[47].

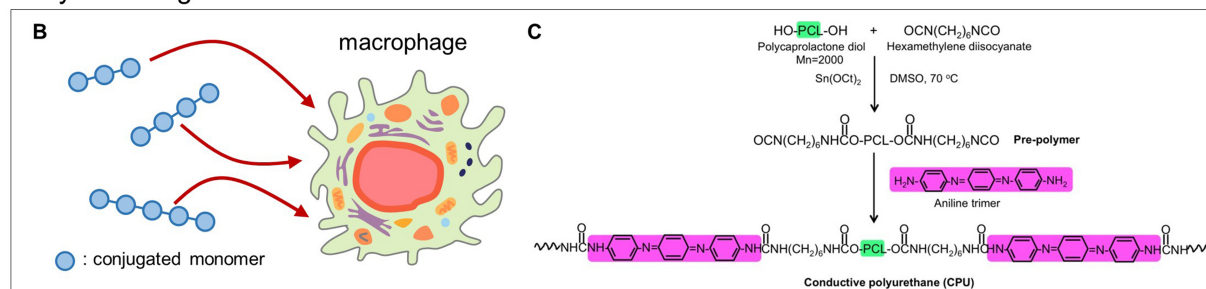
Biologically mediated degradation represents one approach in which organisms facilitate the breakdown of conductive materials. Insects such as *Zophobas morio* (*Z. morio*) and mealworms have demonstrated the ability to metabolize hydrocarbon-based substrates, including materials containing stable C-C bonds^[82]. Moreover, because mealworms cannot ingest rigid polymers but readily consume soft materials, they may enable complete biodegradation of soft conductive polymers^[83,84]. Figure 4A illustrates that a composite based on poly(vinyl alcohol) (PVA) blended with melanin nanoparticles (MNPs) extracted from squid ink exhibits an electrical conductivity of 10⁻¹ S·cm⁻¹ and undergoes ingestion-driven degradation. Optimization of the MNP/PVA ratio enhances the feeding activity of *Z. morio* larvae by up to 5.2-fold^[85]. Furthermore, Fourier transform infrared (FT-IR) analysis of excreta confirms that degradation proceeds beyond physical fragmentation, reaching molecular-level transformation through biological digestion^[29]. Despite these advantages, reliance on biological pathways limits scalability and process control, while the underlying degradation mechanisms remain incompletely understood.

Enzymatic degradation within biological systems provides an alternative route toward complete bioresorption^[13,22,24,26,86-90]. This strategy employs short conjugated oligomers, typically consisting of 2 to 8 thiophene or aniline units, connected via degradable linkers to facilitate macrophage-mediated phagocytosis [Figure 4B]^[24,91-94]. For example, *in vivo* studies^[13] have shown that pyrrole-thiophene-pyrrole-based polymers implanted subcutaneously in rats undergo gradual degradation over 14, 21, and 29 days while eliciting

Ingestible degradation



Enzymatic degradation



Hydrolyzable degradation

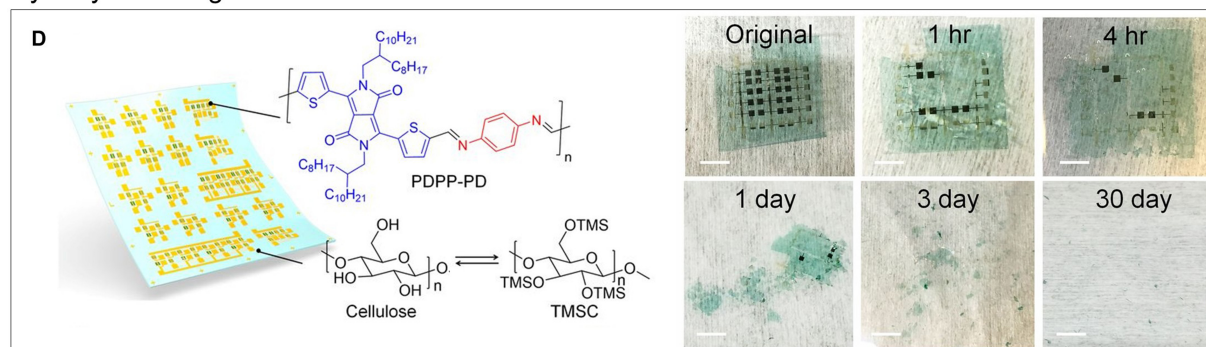


Figure 4. Fully degradable strategies for conductive polymer-based electronics. (A) Schematic illustration of ingestion-driven degradable MNP/PVA composite film fabrication by dispersing squid-ink-derived MNPs in a PVA solution, followed by depletion force-assisted MNP clustering. The photographs on the right show the degradation test setup and the extent of biodegradation of an MNP/PVA film (mass ratio = 2:1) after 12 h. Reproduced with permission from Ref.^[85]. Copyright 2019, John Wiley & Sons; (B) Schematic illustration of macrophage-mediated degradation of conjugated oligomers; (C) Schematic illustration of the two-step polyaddition synthesis of biodegradable conductive polyurethane using PCL, HDI, and aniline trimer. Reproduced with permission from Ref.^[30]. Copyright 2016, John Wiley & Sons; (D) Schematic illustration of a flexible device based on disintegrable semiconducting polymers [p(DPP-PPD)] featuring acid-hydrolyzable imine linkages on an ultrathin biodegradable cellulose substrate. The photographs on the right show the flexible device at various stages of disintegration, demonstrating the degradation process in a pH 4.6 buffer solution containing 1 mg/mL cellulase (scale bars: 5 mm). Reproduced with permission from Ref.^[31]. Copyright 2017, National Academy of Sciences. MNP: Melanin nanoparticle; PVA: poly(vinyl alcohol); PCL: polycaprolactone; HDI: hexamethylene diisocyanate; P(DPP-PPD): poly(diketopyrrolopyrrole-*p*-phenyldiamine); DMSO: dimethyl sulfoxide; TMS: trimethylsilyl; TMSC: trimethylsilyl-functionalized cellulose.

minimal inflammatory responses comparable to those of Food and Drug Administration (FDA)-approved poly(lactic-co-glycolic acid) (PLGA). **Figure 4C** shows that aniline trimers incorporated into a biodegradable polyurethane matrix can maintain approximately 87% of their initial conductivity (10^{-8} - 10^{-5} S·cm⁻¹) over 150 h under humid conditions. Systems incorporating PCL as a soft segment achieve high elasticity, with over 97% instantaneous recovery at 10% strain^[30]. However, the limited fraction of conjugated segments in these materials restricts overall conductivity, thereby limiting their applicability in systems requiring

high-performance charge transport.

Chemical strategies based on dynamic covalent bonds offer additional routes toward fully degradable conductive polymers. Hydrolyzable imine bonds preserve π -conjugation while enabling degradation through reversible bond cleavage^[95]. As shown in **Figure 4D**, diketopyrrolopyrrole (DPP)-based polymers incorporating imine linkages undergo complete degradation within 30 days under mildly acidic conditions (pH 4.6). Through this degradation process, potentially harmful residual species such as aluminum and *p*-phenylenediamine were found to remain well below commonly accepted safety limits, indicating minimal risk to human health and the environment^[31]. Degradation can also proceed under alkaline conditions, depending on polymer composition and environmental factors, as demonstrated in systems that undergo complete clearance in 0.5 M NaOH (pH 13.7)^[96]. However, the requirement for non-physiological pH conditions limits their applicability in biointerfaced environments.

Despite these advances, fully degradable conductive polymers remain constrained by the balance between electrical performance and degradability. Materials designed for complete degradation often rely on specific environmental triggers, whereas systems that operate under broader conditions tend to exhibit reduced conductivity. Further progress will require molecular designs that balance these competing requirements while aligning material properties with appropriate application environments in transient electronic systems.

Applications of biodegradable conductive polymers

Biodegradable conductive polymers enable a wide range of transient bioelectronic applications owing to their mechanical compliance, electronic functionality, and tunable degradation behavior^[97]. These materials have been explored in bioelectrical stimulation platforms^[24,76,90,98], drug delivery systems^[28,54,99-101], sensing devices^[67,73], and active electronic components^[31,102], where soft interfaces and controlled operational lifetimes are essential.

For bioelectrical stimulation, biodegradable conductive polymers are particularly attractive because relatively low conductivity levels are sufficient to elicit cellular responses^[103]. For example, electrospun PLGA/polydopamine (PDA)/CS membranes exhibit a conductivity of $2.85 \times 10^{-3} \text{ S}\cdot\text{cm}^{-1}$, comparable to that of natural skin, and enhance fibroblast proliferation and collagen production under low-voltage stimulation^[98]. These results demonstrate that biodegradable conductive materials can support electrically assisted tissue regeneration while maintaining mechanical properties suitable for soft biointerfaces.

These materials also enable electrically responsive drug delivery systems. Early platforms primarily relied on passive drug release through matrix degradation or diffusion^[104]. For instance, drugs loaded into PGS/PPy composites are gradually released as the biodegradable matrix degrades^[54]. Extending this approach, electrically controlled release systems have also been demonstrated^[28]. **Figure 5A** illustrates a Dex (dextran)-aniline tetramer (AT)/hexamethylene diisocyanate (HDI) conductive hydrogel system that enables on-demand release via electrophoretic transport and redox-induced network contraction. Under electrical stimulation in phosphate-buffered saline (PBS) at 37 °C, dexamethasone release increases by approximately two- to three-fold at applied voltages of 1-3 V, demonstrating electrically controlled therapeutic delivery^[99].

Beyond stimulation and drug delivery, biodegradable conductive polymers also enable mechanically compliant sensing platforms. Their ability to preserve conductive pathways under deformation allows reliable signal transduction in soft and wearable environments^[105]. For example, **Figure 5B** demonstrates a biodegradable composite composed of cellulose nanofibers (CNF), PANI, and natural rubber (NR-8), which has been used to fabricate a strain sensor. The device maintains stable strain sensitivity over approximately 100 loading cycles ($\approx 200 \text{ s}$), demonstrating operational durability^[71]. This performance originates from the

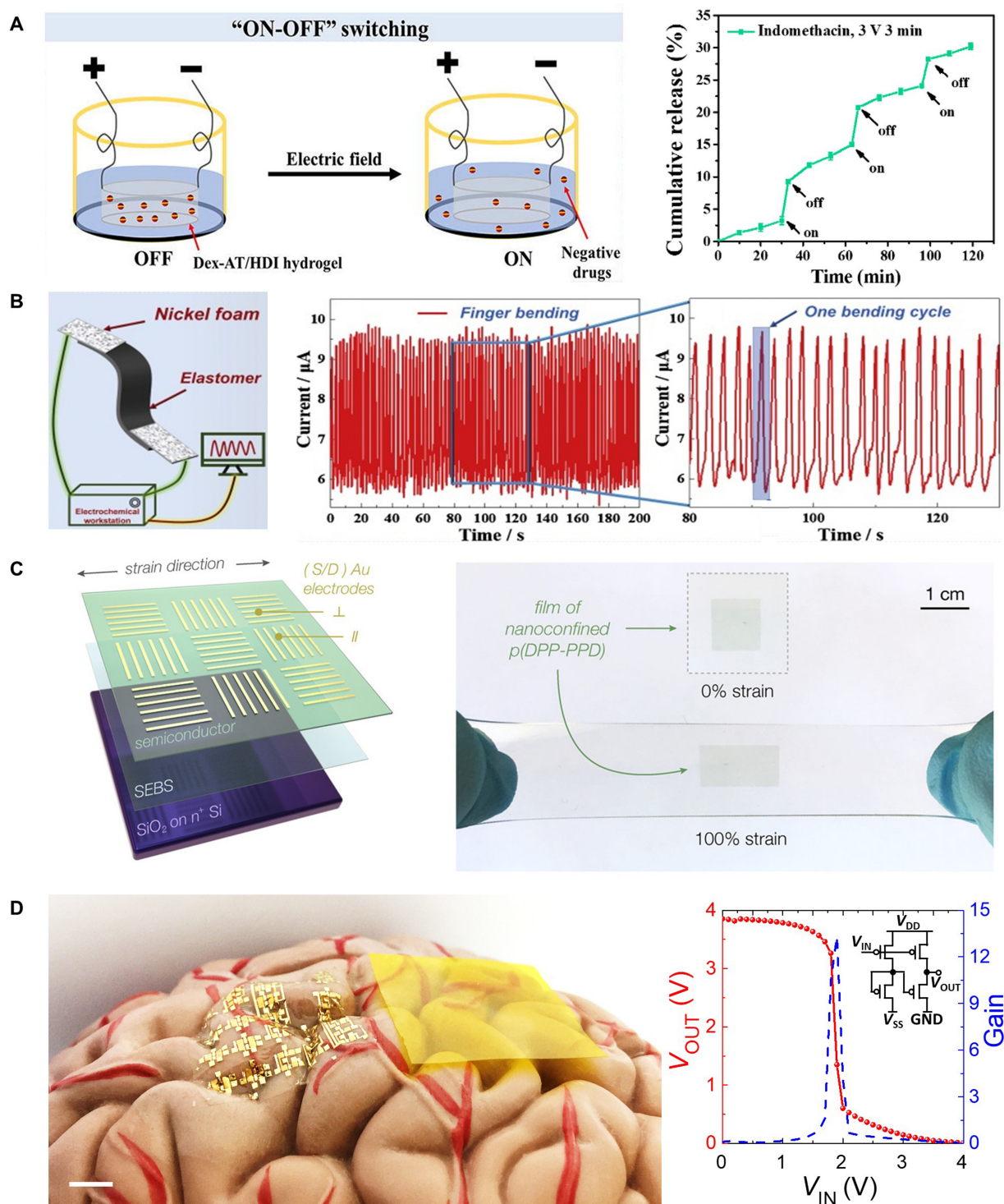


Figure 5. Applications of biodegradable conductive polymers in biomedical and biointerfaced electronics. (A) Schematic illustration of an electro-responsive Dex/HDI conductive hydrogel system for precise on-off drug delivery controlled by external electrical stimuli. The graph on the right shows the drug release profile of indomethacin in phosphate buffer (pH 7.4) under 3 V stimulation (3 min every 30 min). Reprinted with permission from Ref.^[99]. Copyright 2019, Elsevier; (B) Strain sensors based on a CNF-PANI/NR-8 elastomer and nickel foam attached to index fingers for monitoring finger bending. The graph on the right shows the current response during finger motion. Reprinted with permission from Ref.^[71]. Copyright 2019, Elsevier; (C) Schematic illustration of a TFT structure used to evaluate neat and nanoconfined p(DPP-PPD) films under mechanical strain. Bottom: Photographs of nanoconfined p(DPP-PPD) films stretched to 100%. Reproduced with permission from Ref.^[102] under the ACS AuthorChoice license; (D) Left: Photograph of a biodegradable pseudo-CMOS circuit based on p(DPP-PPD), fabricated on a $\sim 25 \mu\text{m}$ -thick PI substrate and placed on a human brain model. The right panel shows the circuit diagrams and corresponding input–output characteristics. Reproduced with permission from Ref.^[31]. Copyright 2017, National Academy of Sciences. Dex: Dextran; HDI: hexamethylene diisocyanate; CNF: cellulose nanofiber; PANI: polyaniline; NR: natural rubber; TFT: thin-film transistor; P(DPP-PPD): poly(diketopyrrolopyrrole-*p*-phenyldiamine); CMOS: complementary metal-oxide-semiconductor; PI: polyimide; AT: aniline tetramer; SEBS: polystyrene-block-poly(ethylene-*ran*-butylene)-block-polystyrene.

CNF-derived framework, while the elastic NR matrix preserves conductive pathways during repeated deformation^[71]. This concept also extends to pressure sensing, where Gel-g-P3HT aerogel films exhibit pressure-dependent current responses under applied pressures of 5–20 kPa^[73]. These results demonstrate that biodegradable conductive polymers provide mechanically compliant sensing platforms suitable for wearable and biointegrated applications.

Biodegradable conductive polymers have also been extended to active electronic devices that require controlled charge transport and signal modulation^[106]. Early work by IrimiaVladu and colleagues demonstrated fully biodegradable organic transistors composed of degradable substrates, dielectrics, and semiconducting layers^[107]. However, these systems often relied on externally degradable components rather than intrinsically degradable semiconductors, prompting subsequent efforts to develop molecularly engineered biodegradable semiconducting materials. **Figure 5C** illustrates a degradable and stretchable semiconductor system based on a highly extensible urethane-based E-PCL elastomer matrix combined with the organic semiconductor poly(diketopyrrolopyrrole-*p*-phenyldiamine) [p(DPP-PPD)]. Optimized side-chain engineering of p(DPP-PPD) using branched alkyl substituents improves compatibility with the elastomer matrix and suppresses macroscopic aggregation^[102]. This design promotes nanoscale phase separation, forming nanoconfined semiconducting domains that suppress crystallization and delay crack initiation^[102]. As a result, the composite maintains crack-free film integrity under mechanical deformation. A film composed of 70% E-PCL and 30% p(DPP-PPD) retains semiconducting performance even at 100% strain, with a mobility of approximately $0.05 \text{ cm}^2 \cdot \text{V}^{-1} \cdot \text{s}^{-1}$ ^[102]. These results highlight the potential of biodegradable semiconductors for stretchable and skin-inspired electronics^[102]. **Figure 5D** presents the integration of degradable semiconductors into transient logic circuits. Fully degradable ultrathin devices fabricated by integrating acid-hydrolyzable p(DPP-PPD) on cellulose substrates exhibit lightweight structures that can be supported by a human hair and show less than 5% variation in transfer characteristics under bending^[31]. Pseudo-CMOS inverters demonstrate a noise margin of 1.2 V with sharp switching behavior, while NAND and NOR circuits achieve near rail-to-rail voltage swings^[31]. These demonstrations illustrate that biodegradable semiconductors can support flexible logic circuits and enable more complex transient electronic functionalities^[31].

Collectively, these examples illustrate the broad potential of biodegradable conductive polymers across tissue engineering, drug delivery, sensing, and active electronics. However, their relatively low intrinsic conductivity remains a key limitation for applications requiring reliable charge transport in interconnects, electrodes, and circuit-level integration. In addition, achieving complete biodegradation under physiological conditions remains challenging. Addressing these challenges will require continued advances in molecular design and materials engineering to further enable high-performance, fully transient bioelectronic systems.

FULLY BIODEGRADABLE CONDUCTIVE COMPOSITE PASTES

The defining characteristic of conductive composite pastes lies in their filler-matrix architecture, including the dispersion state of metallic fillers within a mechanically compliant polymer matrix. The polymer matrix ensures mechanical compatibility with soft biological tissues, while the metallic fillers form percolating networks that prevent complete loss of electrical conductivity even under dynamic deformation such as stretching and bending^[33]. Compared with conventional thin-film structures, composite pastes reduce processing complexity and offer scalable routes for large-area manufacturing^[108]. Furthermore, this filler-matrix configuration provides design flexibility distinct from that of thin-film conductors. Its high compatibility with solution-based printing techniques such as screen printing^[12], electrospinning^[109], and 3D printing^[110], enables the fabrication of electrodes and interconnects with complex geometries.

Table 4. Percolation parameters and optimum filler loadings of various biodegradable conductive composites

Composite	Critical volume fraction [vol.%]	Critical exponent	Optimum volume fraction [vol.%]	Optimum conductivity [$S \cdot m^{-1}$]
Mo/PBTPA ^[111]	20	1.6	35	-1,400
Mo/PBAT ^[33]	20	0.9	35	1,400, 1,800*
Mo/PCL ^[12]	5	0.6	30	1,078-1,454*
Mo/candelilla wax ^[112]	17	1.9	30	-1,000
W/beeswax ^[35]	19	1.6	27	-6,400, -7,200**

*Addition of tetraglycol as a filler dispersant. **Addition of glycofurol as a filler dispersant. PBTPA: Poly(1,4-butanedithiol-co-1,3,5-triallyl-1,3,5-triazine-2,4,6(1H,3H,5H)-trione-co-4-pentenoic anhydride); PBAT: poly(butylene adipate-co-terephthalate); PCL: polycaprolactone.

Notably, compared with conjugated-polymer-based conductors, these composite systems can enable complete biodegradation under physiological conditions while maintaining superior electrical conductivity and mechanical flexibility, making them particularly attractive for minimally invasive bioelectronic applications. To achieve composite biodegradability, both the matrix and the conductive fillers are typically selected from materials that decompose into non-toxic byproducts under physiological or environmental conditions. Biodegradable polymer matrices primarily include synthetic polyesters such as poly(butylene adipate-co-terephthalate) (PBAT)^[33], poly(1,4-butanedithiol-co-1,3,5-triallyl-1,3,5-triazine-2,4,6(1H,3H,5H)-trione-co-4-pentenoic anhydride) (PBTPA)^[111], PCL^[12], PLA^[32], and PLGA^[111], as well as natural materials like wax^[112] and silk fibroin^[34]. These matrices serve to mechanically support the fillers and protect them from the external environment while simultaneously dictating the overall flexibility, stretchability, and degradation kinetics of the composite system. Regarding the conductive phase, biodegradable metallic fillers such as zinc (Zn)^[113], iron (Fe)^[114], tungsten (W)^[108], and molybdenum (Mo)^[12] are predominantly utilized. The electrical performance of these biodegradable pastes is governed by percolation theory, in which a continuous conductive network forms as filler particles interconnect at a critical volume fraction, known as the percolation threshold^[115,116]. For instance, the percolation threshold of Mo/PBTPA composites has been reported to occur at approximately 20 vol%^[111]. According to percolation theory [see Equation (1)], the electrical conductivity of the composite improves as the conductive filler fraction increases.

$$\sigma = \sigma_0(\varphi - \varphi_c)^t, \quad (1)$$

Specifically, beyond the critical volume fraction (φ_c), the connectivity of the conductive phase is reinforced as the filler fraction (φ) increases, and the composite conductivity (σ) scales with the scaling factor (σ_0) and the critical exponent (t). However, at high filler loadings, filler particles often fail to disperse uniformly within the matrix, leading to agglomeration. This phenomenon not only compromises the integrity of the conductive network but also significantly reduces the mechanical flexibility of the composite^[33]. Furthermore, increasing the filler fraction enhances the viscoelasticity of the composite, presenting a significant challenge for practical manufacturing processes such as printing or coating^[12]. In the case of Mo/PBAT^[33] and Mo/PCL^[12] systems, optimal conductive networks were found to form at volume fractions of approximately 35 vol% and 30 vol%, achieving electrical conductivities of 1,400 and $1,266 \pm 188 S \cdot m^{-1}$, respectively [Table 4].

Despite the significant potential of biodegradable conductive composite pastes in the field of biointerfaced electronics, a notable discrepancy persists between their biodegradation behavior and functional reliability. Ideally, transient composite conductors are designed to safely disappear from the body after fulfilling a specific clinical mission; however, their actual operational stability often degrades much faster than intended^[111]. Therefore, it is imperative to maintain stable electrical and mechanical performance throughout

Table 5. Degradation kinetics of individual biodegradable inorganic fillers and polymer matrices

Materials	Dissolution conditions			Electrical dissolution rates [nm·h ⁻¹]	
	Solution type	pH	Temperature [°C]		
Filler	Mo	DI water	7	RT	1 ^[117]
	W	DI water	7	RT	3-5 ^[117]
	Fe	DI water	7	RT	1 ^[117]
	Zn	DI water	7	RT	50-90 ^[117]
	Mg	DI water	7	RT	200-400 ^[117]
					Degradation rate [wt.% day ⁻¹]
Matrix	PBTPA	PBS	7.4	37	0.08-0.1 ^[118]
	PCL	Soil	-	30	0.03 ^[119]
	PLA	PBS	7.25	37	0.07-1 ^[120]
	PLGA	PBS	7.4	37	0.3-2 ^[121]
	PBAT	Lipase	-	50	0.38-0.54 ^[122]
	Beeswax	Compost	-	40	0.76 ^[123]
	Candelilla wax	Compost	-	40	0.05 ^[123]
	Silk fibroin	PBS	7.4	37	0.17-0.34 ^[124]

DI: Deionized; RT: room temperature; PBTPA: poly(1,4-butanedithiol-co-1,3,5-triallyl-1,3,5-triazine-2,4,6(1H,3H,5H)-trione-co-4-pentenoic anhydride); PBS: phosphate-buffered saline; PCL: polycaprolactone; PLA: polylactic acid; PLGA: poly(lactic-co-glycolic acid); PBAT: poly(butylene adipate-co-terephthalate).

the operational lifetime of the device before rapid and complete dissolution occurs. Such design strategies enhance the moisture resistance of wearable devices, enabling continuous monitoring without performance degradation caused by sweat or ambient humidity. They also allow implantable devices to maintain stable performance until their intended mission is completed, after which they are fully resorbed by the body. This section reviews material design strategies aimed at preserving the functional stability of biodegradable conductive paste materials throughout their operational lifetimes and discusses approaches for extending these materials to various transient bioelectronic applications.

Material design strategies for the functional reliability of biodegradable conductive composite pastes

To precisely design the practical operational lifetime of composite devices, it is essential to quantitatively characterize the degradation kinetics of both the individual constituents and the resulting composites. First, biodegradable metals primarily used as conductive fillers undergo chemical dissolution following surface oxidation in aqueous environments. For example, Mo, Fe, and W thin films exhibit gradual electrical dissolution rates of approximately 1 nm·h⁻¹ (for Mo^[117] and Fe^[117]) and 3-5 nm·h⁻¹ (for W^[117]) in deionized (DI) water at room temperature, thereby maintaining relatively stable conductivity [Table 5]. In contrast, Zn^[117] and Mg^[117] thin films exhibit significantly higher corrosion rates of 50-90 and 200-400 nm·h⁻¹, respectively [Table 5], which makes them challenging to use as stable fillers because of their rapid disintegration. The degradation of these fillers is accelerated as water-soluble oxides or hydroxides formed on the surface diffuse into the surrounding biofluids^[125].

Polymer matrices also exhibit diverse degradation profiles depending on their chemical structures and components. Synthetic polyesters such as PBTPA (0.08-0.1 wt.% day⁻¹)^[118], PCL (0.03 wt.% day⁻¹)^[119], PLA (0.07-1 wt.% day⁻¹)^[120], PLGA (0.3-2 wt.% day⁻¹)^[121], and PBAT (0.38-0.54 wt.% day⁻¹)^[122] degrade primarily through the hydrolysis of ester bonds in their polymer backbones [Table 5]. Natural waxes, including beeswax (0.76 wt.% day⁻¹)^[123] and candelilla wax (0.05 wt.% day⁻¹)^[123], exhibit gradual degradation behavior due to their high water resistance. Meanwhile, the natural protein silk fibroin (0.17-0.34 wt.% day⁻¹)^[124]

Table 6. Functional lifetimes and structural parameters of various biodegradable conductive composite pastes

Composite	Dissolution conditions			Functional lifetime	Paste Thickness (μm)	Filler size (μm)
	Solution type	pH	Temperature [$^{\circ}\text{C}$]			
Mo/PBTPA	PBS	7.4	37	9 ^[111]	190	1-5
Mo/PLGA	PBS	7.4	37	-4 ^[111]	190	1-5
Mo/PLLA	PBS	7.4	37	-3 ^[111]	190	1-5
Mo/PCL	PBS	7.4	37	-10 ^[12]	100	1-2
Mo/PCL@PPC*	PBS	7.4	37	> 10 ^[11]	-	2.54
Mo/candelilla Wax	PBS	7.4	37	19 ^[12]	50	< 5
Mo/PBAT	PBS	7.4	37	>16 ^[33]	500-1,000	5-100
W/PLA	RO water	7	37	> 7 ^[32]	-	6-12
W/beeswax	PBS	7.4	37	13 (> 13**) ^[35]	200	0.5
W/silk fibroin	PBS	7.4	95	-2 ^[34]	150	10
W/PBAT@PBTPA	PBS (lipase)	7.4	50	15 ^[108]	450	10

*Encapsulated with a PPC layer. **Functional lifetime exceeds 13 days with the addition of glycofuran. PBTPA: Poly(1,4-butanedithiol-co-1,3,5-triallyl-1,3,5-triazine-2,4,6(1H,3H,5H)-trione-co-4-pentenoic anhydride); PBS: phosphate-buffered saline; PLGA: poly(lactic-co-glycolic acid); PLLA: poly(L-lactic acid); PCL: polycaprolactone; PPC: poly(propylene carbonate); PBAT: poly(butylene adipate-co-terephthalate); PLA: polylactic acid; RO: reverse osmosis.

degrades through proteolysis, in which amide bonds are cleaved by specific enzymes [Table 5].

Unlike conventional pastes using stable hydrophobic polymers (e.g., epoxy, silicone elastomer)^[126,127] and chemically inert noble metal fillers (e.g., silver, gold)^[126,128], biodegradable conductive composites exhibit rapid initial functional degradation within physiological environments. Despite these individual degradation rates, the actual functional lifetime of these composite pastes is typically limited to approximately 2 to 19 days [Table 6]^[11,12,32-35,108,111,112]. Considering the typical filler size (0.5–100 μm) and paste thickness (50–1,000 μm), this operational duration is markedly shorter than the time required for complete dissolution of the components^[11,12,32-35,108,111,112]. The root cause of this premature functional failure lies in the extreme structural sensitivity of the percolation network in aqueous environments, which disrupts physical contact or the critical quantum tunneling distance between fillers, both of which are essential for maintaining electrical integrity^[111]. As a result, the functional stability of biodegradable composites is often governed more by early microstructural disruption of the filler percolation network than by the overall mass loss of the constituent materials. In other words, predicting the lifetime of the composite requires an approach that considers filler dispersion, interfacial stability, and water diffusion behavior rather than simply comparing the dissolution rate of metallic fillers or the mass loss rate of the polymer matrix. These characteristics highlight the importance of design strategies that preserve electrical connectivity throughout the intended operational lifetime before the onset of rapid transient degradation.

Figure 6A illustrates the microstructural evolution of Mo-based biodegradable conductive composites in a physiological-mimicking environment (PBS, 37 $^{\circ}\text{C}$) as a function of the matrix type^[111]. The lower series, corresponding to the Mo/PLGA composite, shows a rapid decline in electrical performance over time. This behavior is mainly associated with the hydrophilic nature of the PLGA matrix, which promotes water uptake and swelling, thereby weakening the filler–matrix interface and leading to interfacial debonding^[111]. Previous studies report that PBS preferentially infiltrates the vulnerable interfaces between Mo particles and the PLGA matrix. The resulting expansion of localized voids physically disrupts the percolation pathways well before the metallic fillers undergo significant dissolution, leading to a sharp decrease in conductivity^[111]. By contrast, the upper series representing the Mo/PBTPA composite maintains stable conductivity for more than one

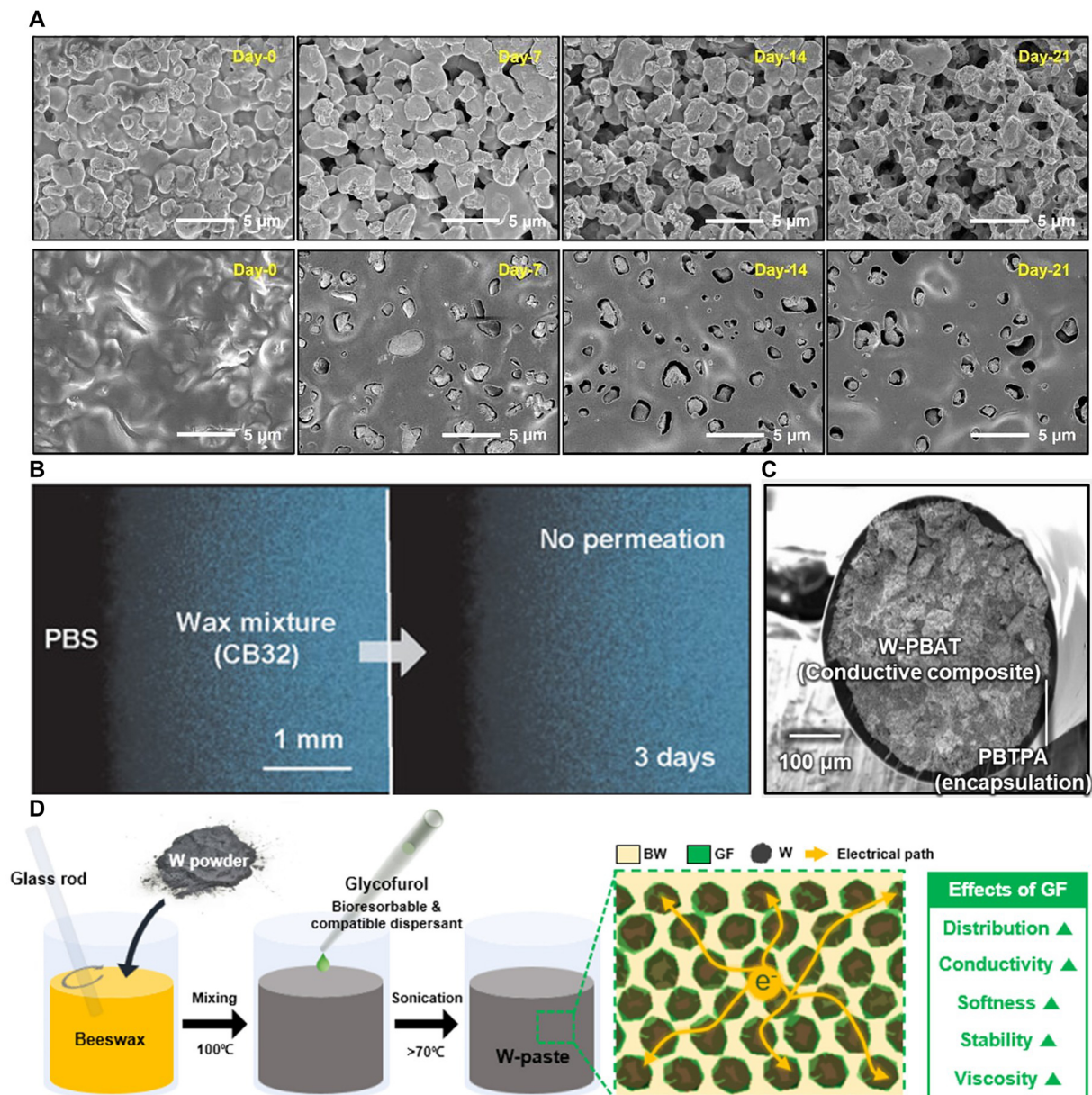


Figure 6. Strategies for maintaining the operational stability of biodegradable conductive composite pastes against degradation. (A) Comparative analysis of microstructural changes during immersion, presenting a series of SEM images of Mo/PBTAPA paste (top) and Mo/PLGA paste (bottom) in PBS at 37 °C. The images contrast the degree of surface erosion and pore formation over time. Reprinted with permission from Ref.^[111]. Copyright 2018, Elsevier; (B) Optical images demonstrating the waterproofing efficacy of the wax mixture layer, showing effective inhibition of internal penetration even after 3 days under physiological conditions (37 °C, pH 7.4). Reproduced with permission from Ref.^[129]. Copyright 2020, John Wiley & Sons; (C) SEM image of a one-dimensional W/PBAT conductive composite fiber encapsulated with a PBTPA polymer coating to prevent premature environmental degradation. Reproduced with permission from Ref.^[108] under the CC BY license; (D) Schematic illustration of the fabrication process for W/beeswax pastes with the addition of GF as a dispersant, detailing enhanced particle dispersion and the resulting overall stability of the composite. Reproduced with permission from Ref.^[35] under the CC BY-NC-ND license. No modifications were made. SEM: Scanning electron microscopy; PBTPA: poly(1,4-butanedithiol-co-1,3,5-triallyl-1,3,5-triazine-2,4,6(1H,3H,5H)-trione-co-4-pentenoic anhydride); PLGA: poly(lactic-co-glycolic acid); PBS: phosphate-buffered saline; PBAT: poly(butylene adipate-co-terephthalate); GF: glycofural; BW: beeswax.

week^[111]. PBTPA is a highly hydrophobic polymer that forms strong interfacial interactions with the native hydrophobic oxide layer (MoO_3) present on the Mo surface. This interfacial compatibility promotes uniform filler dispersion and suppresses void formation under aqueous exposure^[111]. As a result, the conductive network remains structurally stable because water infiltration along the filler–matrix interface is significantly reduced, allowing sustained electrical performance over extended periods^[111].

Since functional failure typically originates from the infiltration of physiological fluids^[125], matrix designs that limit water diffusion are important for preserving the conductive network. **Figure 6B** presents an optical analysis of water infiltration at the silicon–wax interface, showing no visible penetration into the wax layer for up to 3 days at 37 °C in PBS (pH 7.4)^[129]. This behavior arises from the high hydrophobicity and crystallinity of natural wax, which provide low moisture permeability and strong resistance to swelling. These moisture-barrier characteristics are associated with extended functional lifetimes^[129]. Specifically, the Mo/candelilla wax composite has been reported to maintain stable conductivity for up to 5 days at 37 °C in PBS, with complete electrical disconnection occurring only after approximately 19 days^[112]. Although irreversible water diffusion and eventual network collapse cannot be entirely avoided, such matrix design strategies can substantially prolong the operational lifetime of the conductive composite within the intended transient window.

Beyond matrix design, encapsulation strategies that introduce an additional protective layer provide an effective approach to improving functional reliability by delaying water diffusion and suppressing premature filler corrosion^[108]. **Figure 6C** shows a cross-sectional scanning electron microscopy (SEM) image of a W/PBAT composite fiber conductor encapsulated with a PBTPA coating^[108]. This structural protection enables the fiber to maintain strong chemical durability, exhibiting a conductivity change of less than 2% even after 20 washing cycles under various pH conditions^[108]. Similarly, Mo/PCL composite fibers coated with poly(propylene carbonate) (PPC) retain stable resistance for up to 10 days, whereas uncoated counterparts fail within 2 days^[11]. These observations highlight the role of encapsulation in extending the functional stability of conductive composites under practical operating conditions.

In addition to physical coatings, dispersants can enhance reliability by controlling the microstructure of the composite^[12,33,35]. **Figure 6D** schematically illustrates the fabrication process and functional stability of a W/beeswax conductive paste containing glycofurol (GF). When immersed in PBS at 37 °C, the GF-containing composite preserves its initial conductivity for approximately 13 days, even after two weeks of exposure^[35]. This behavior is associated with the role of GF in promoting uniform filler dispersion and modulating the surface tension of the paste, thereby stabilizing interfacial interactions within the percolation network^[35]. In contrast, additive-free control samples develop cracking that rapidly disrupts conductive pathways, leading to early electrical failure^[35].

In summary, the reliability of biodegradable conductive composites is achieved through the strategic selection of hydrophobic matrices, the integration of protective encapsulation layers, and interface optimization via dispersants. This multifaceted engineering approach provides a critical design foundation for ensuring that devices operate with stable reliability for a programmed duration, even under the harsh conditions of biological environments.

Biodegradable conductive composite paste-based sensors and devices

Biodegradable flexible conductive composite systems integrated into bio-interfaced electronics offer several advantages over conventional biodegradable conductive polymers, particularly complete biodegradability and reduced interfacial impedance resulting from their higher electrical conductivity^[12]. As discussed in Section “Material design strategies for the functional reliability of biodegradable conductive composite pastes”, combinations of matrices and conductive fillers provide the basis for maintaining functional reliability and programming device operational lifetimes. Owing to their fluidic processability and mechanical compliance, these composite pastes can be integrated into a wide range of biointerfaced electronic platforms, including transient interconnects^[35,111], sensors^[11,33,34], textile-integrated electronics^[108], and wireless implantable stimulators^[11,12].

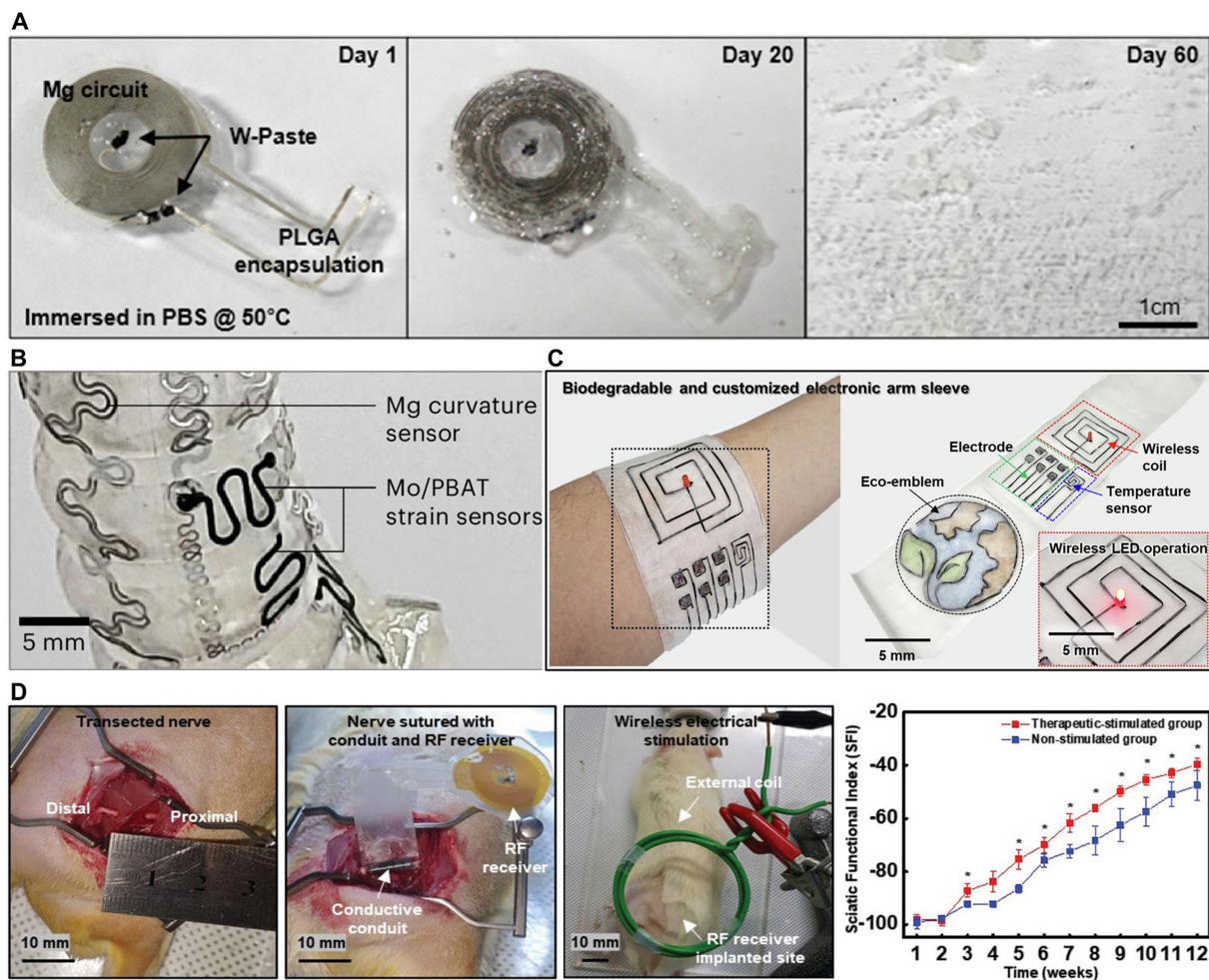


Figure 7. Applications of biodegradable conductive pastes in biointerfaced systems. (A) Images of a bioresorbable wireless power-harvesting and stimulation device in which tungsten paste (W-paste) serves as the interconnection material, exhibiting a programmed operational lifetime. Reproduced with permission from Ref.^[35] under the CC BY-NC-ND license. No modifications were made; (B) Mo/PBAT strain sensor integrated onto a fully compostable soft robotic finger. Reproduced with permission from Ref.^[131]. Copyright 2026, Springer Nature; (C) Biodegradable electronic arm sleeve system fabricated from W/PBAT fibers. Reproduced with permission from Ref.^[108] under the CC BY license; (D) Biodegradable Mo/PCL composite nerve interface: (left) surgical procedure for implantation and (right) functional recovery of the sciatic nerve assessed via SFI. Reproduced with permission from Ref.^[12] under the CC BY license. PBAT: Poly(butylene adipate-co-terephthalate); PCL: polycaprolactone; SFI: sciatic functional index; PLGA: poly(lactic-co-glycolic acid); PBS: phosphate-buffered saline; LED: light-emitting diode; RF: radio frequency.

Figure 7A illustrates the use of a W/bee wax conductive paste as an electrical interconnect in bioresorbable electronics, maintaining a stable electrical pathway during device operation and subsequently disappearing after the intended functional lifetime. This paste, characterized by a high conductivity exceeding $7 \text{ kS}\cdot\text{m}^{-1}$, exhibits electrical properties comparable to those of conventional non-bioresorbable silver epoxy, thereby minimizing potential performance fluctuations or interfacial instabilities in bioresorbable electronics^[35]. In a separate study, similar performance characteristics were also observed in wireless stimulators employing W/candelilla wax paste as interconnects, which maintained stimulation voltages up to 30 V and exhibited excellent mechanical flexibility under deformation^[130]. In addition to functioning as compliant interconnects that buffer interfacial stress during mechanical deformation, these composite pastes can also serve as passive electronic components such as resistors^[112], capacitors^[112], and inductors^[33].

Composite pastes can also function as conformal sensors integrated with soft robotic systems^[131] or biological systems^[34]. **Figure 7B** presents a Mo/PBAT-based strain sensor attached to the surface of a fully compostable

soft robotic finger^[131]. These conductive pastes are employed to ensure stable electrical interfaces while accommodating the high mechanical flexibility required for soft systems. Owing to its low bending stiffness, the flexible sensor closely conforms to the surface of a PGS-based soft robot and exhibits stable resistance changes at strains up to 80%^[131]. Stable electronic performance is maintained even under large mechanical deformation, after 2,000 cycles of repeated deformation, and following 4 months of storage^[131]. The non-toxic degradation by-products serve as nutrient sources, activating soil enzymes and supporting plant growth, allowing the system to return naturally to the ecosystem after use^[131]. Beyond strain sensing, similar composite systems have been used to realize temperature^[11,33,108] and physiological signal^[34] monitoring for bio-interfaced applications.

These materials can also be processed into one-dimensional fibers through drawing or spinning^[11,108], enabling seamless integration with conventional textile manufacturing. As illustrated in Figure 7C, a smart arm sleeve was fabricated by stitching PBTPA-coated W-PBAT composite fibers onto a biodegradable PLA fabric, enabling the integration of temperature sensors, electromyography (EMG) electrodes, and inductive coils for wireless power transfer^[108]. The EMG electrodes exhibit an interface impedance of 26.20 ± 8.71 k Ω at 1 kHz, enabling the detection of electromyographic signal changes during limb movement, even in the absence of conductive gels^[108]. This impedance profile corresponds to a signal-to-noise ratio (SNR) of 8.80 ± 0.49 dB, supporting the observation of neuromuscular coordination patterns^[108]. Within this context, physiological signals can be monitored in real time, including a 2 °C increase in skin temperature during running^[108]. The entire textile system decomposed naturally in soil within approximately 120 days^[108], highlighting the potential of these materials for environmentally sustainable wearable electronics.

Biodegradable composite conductors can also be utilized in fully implantable therapeutic systems^[12]. Figure 7D shows the implantation of a wireless radio-frequency receiver and a conductive nerve conduit (CNC) platform in a 10 mm sciatic nerve defect model, illustrating a system that eliminates infection risks associated with wired external connections. Specifically, the Mo/PCL conduit exhibits a high electrical conductivity of 7.4 S·cm⁻¹, which significantly exceeds the ranges typically reported for conventional conductive polymer or carbon-based materials (10^{-6} to 1.57×10^{-2} S·cm⁻¹)^[12]. This level of electrical performance provides a low-impedance environment, facilitating the consistent transmission of therapeutic signals across the nerve gap. Following daily monophasic pulse stimulation (100 μ s pulse width, 20 Hz, three times per day), the stimulated group achieved a sciatic functional index (SFI) of -39.58 ± 2.36 after 12 weeks, demonstrating improved functional recovery compared with both the unstimulated group (-47.56 ± 5.48) and the autograft control (-43.6 ± 2.5)^[12]. These results suggest that the wireless stimulation platform, which combines high conductivity with mechanical flexibility, effectively supports axonal regeneration and functional recovery in damaged peripheral nerves.

In summary, biodegradable conductive composite systems combine high electrical performance with mechanical compliance compatible with biological tissues. Their versatility - from conformal wearable sensors to fully implantable wireless stimulators - offers a promising pathway toward bioelectronic systems that minimize long-term environmental impact. Continued advances in lifetime control, reliability engineering, and multifunctional integration will further expand the scope of sustainable biointegrated electronics.

MATERIALS DESIGN AND APPLICATIONS OF BIODEGRADABLE OMIECS

OMIECs are central to bioelectronics because they support simultaneous ionic and electronic transport, enabling efficient signal transduction in aqueous and biologically relevant environments^[36]. Reversible ion-driven doping and dedoping enable semiconductor-like switching, making OMIECs particularly suitable for organic electrochemical transistors (OECTs)^[132]. In these devices, ions penetrate into the channel bulk

and modulate conductivity, resulting in volumetric capacitance, high transconductance, and low-voltage operation^[36]. These features make OMIECs attractive for biosignal sensing and neuromorphic bioelectronics^[132]. Furthermore, leveraging these electrochemical ion–electron coupling properties, an integrated sensing–actuation system capable of simultaneous low-voltage operation and real-time strain detection has recently been reported^[31,40,133]. However, conventional OMIECs typically combine ionic and electronic components that exhibit limited or mismatched biodegradability. As summarized in [Table 7](#), biodegradable OMIEC research has therefore evolved from composite-based approaches toward molecular designs that directly incorporate degradability into ionic or electronic components. Importantly, these strategies influence not only degradation behavior but also water stability, ion transport, and device performance.

Early efforts focused on blending established but non-biodegradable OMIECs such as poly(3,4-ethylenedioxythiophene):poly(styrenesulfonate) (PEDOT:PSS) with biodegradable matrices^[29,40,134]. In these systems, biodegradability arises primarily from the surrounding biodegradable matrix, while the conjugated conductor remains largely intact. Representative examples include PEDOT:PSS/sericin composites^[40], which exhibited protease-mediated degradation and were applied to biosensors, and PEDOT:PSS/montmorillonite (MMT)^[29], which demonstrated eco-biodegradation through superworm ingestion. PEDOT:PSS/melanin^[134] provides another example, as melanin not only serves as a bio-derived component but also enhances proton conduction and ionic–electronic coupling, resulting in improved transconductance. These studies demonstrated that biodegradable or bio-derived components can be incorporated into OMIEC platforms without compromising device performance. However, non-covalent blending often leads to phase separation, inhomogeneous films, and incomplete degradation of the conducting phase. Consequently, composite strategies remain limited as a general route toward fully biodegradable OECT channel materials.

To address these limitations, covalent molecular design strategies have been developed to link degradability directly to semiconducting components. One representative example is P(CL-*co*-AVL)-*g*-O₃HT, in which an oligo(3-hexylthiophene) (O₃HT) unit is grafted onto a biodegradable PCL backbone^[137]. Although the PCL-based backbone provides limited ionic conductivity, it supports OECT operation with drain currents in the milliamperage range^[137]. The grafted material fragmented in 2 M trifluoroacetic acid and completely disintegrated in 2 M NaOH, whereas pristine O₃HT showed minimal degradation^[137]. Corresponding OECT devices exhibited a ~70% decrease in performance after 3 days in NaOH and complete failure after 7 days [[Figure 8A](#)]. These results demonstrate that molecular design can introduce degradability into hydrophobic semiconducting systems while preserving device operation. However, degradation was primarily observed under accelerated conditions, and oligomeric fragments persisted, indicating incomplete breakdown.

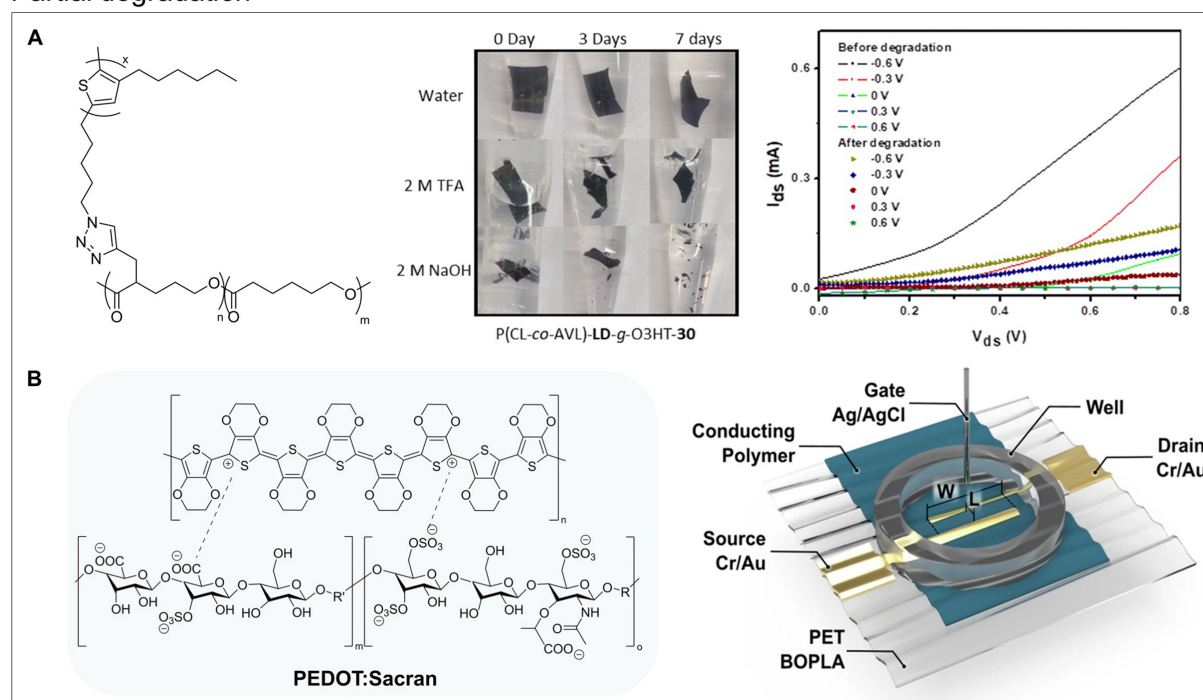
Another major strategy has been to replace the conventional ionic conductor with biodegradable polyelectrolytes, particularly naturally derived anionic polysaccharides listed in [Table 8](#). High-molecular-weight ionic conductors strongly influence key OMIEC properties, including ionic conduction, charge compensation, and aqueous-film stability^[36], while polysaccharides provide hydrolyzable glycosidic bonds for biodegradation and anionic moieties^[143] for ionic conduction and charge compensation. PEDOT polymerization in biodegradable polyelectrolyte matrices enables OMIECs suitable for bioactive dopants, hydrogel scaffolds, neural interfaces, and OECTs [[Table 7](#)]. Among these systems, PEDOT:Sacran represents a particularly promising example. Sacran is an ultrahigh-molecular-weight polysaccharide containing sulfate and carboxylate groups^[38]. Zeta potential analysis suggests a PEDOT:PSS-like core–shell structure that supports efficient ionic–electronic coupling^[38]. Unlike many swellable polysaccharide systems, PEDOT:Sacran provides sufficient water stability for thin-film OECT operation, with a conductivity of 1.18 S·cm⁻¹ and a normalized transconductance of 0.11 S·cm⁻¹^[38] [[Table 7](#)]. Flexible PEDOT:Sacran OECTs on

Table 7. Biodegradable OMIEC-based depletion- and accumulation-mode OECTs

Driving mode	Material	Degradation component	Degradation condition	OMIEC properties			Applications
				Conductivity (S·cm ⁻¹)	Normalized transconductance g _m (NR) (S·cm ⁻¹)	On/off ratio	
Depletion	PEDOT:PSS/Melanin ^[134]	Melanin	-	2 ± 1	51.7	1.8 × 10 ³	OECT supercapacitor
	PEDOT:PSS/Sericin ^[40]	Sericin	Protease (in PBS, 37 °C)	10 ⁻¹	-	-	Biosensor
	PEDOT:PSS/MMT ^[29]	MMT	Superworms hydrated feeding (30 °C)	16.0 ± 0.9	-	-	-
	PEDOT:HA ^[41]	HA	-	1.0–8.0 × 10 ⁻¹	-	-	Bioactive dopant
	PEDOT:chondroitin sulfate	Chondroitin sulfate	-	1.0–10.0 × 10 ⁻¹	-	-	
	PEDOT:HEP	HEP	-	10.0–41.0 × 10 ⁻¹	-	-	
	HA-grafting-PEDOT ^[135]	HA	Intracardiac injection (rat model)	0.56	-	-	Hydrogel scaffold
	Chondroitin sulfate-grafting-PEDOT	Chondroitin sulfate		0.07	-	-	
	HEP-grafting-PEDOT	HEP		1.65	-	-	
	PEDOT:DS ^[36]	DS	-	7–20	-	-	Bioactive dopant
PEDOT:CMCS ^[39]	CMCS	Sodium azide and lysozyme (in PBS, 37 °C)	4.68 ± 0.28 × 10 ⁻³	-	-	Neural tissue engineering	
PEDOT:S-CNCs ^[44]	S-CNCs	-	5	2.13	84	OECT	
PEDOT:Sacran ^[38]	Sacran	Proteinase K [in 0.05 M PBS (pH 8), 37 °C]	1.18	0.11	38 ± 13	Flexible OECT	
PEDOT:LigS ^[43]	LigS	Wetted-soil burial (50 °C)	1.1 ± 0.43	0.21	91 ± 43	Wood-based OECT	
Accumulation	P(CL-co-AVL)-LD-g-O3HT-30 ^[137]	PCL	2 M TFA / 2 M NaOH (in DI water)	5.6 × 10 ⁻³	-	-	OECT
	<i>o</i> -3gTIT ^[46]	Imine bond and oligomer	HFIP (0.05 mg/mL) + TFA (10 vol%), (60 °C)	-	6.7	-	OECT based-inverter OECT based-artificial synapse
	<i>i</i> -3gTIT			-	86.2	-	
	p(DPP _{C12TEG} -TIT) ^[45]	Imine bond and oligomer	0.5 M TFA / 0.1 M HCl (in DI water)	-	0.24 ± 0.18	10 ²	OECT
	p(DPP _{BTEG} -TIT)			-	0.25 ± 0.017	10 ²	Bioelectronics
p(DPP _{C12TEG} -TVT) ^[45]	DPP lactam ring	0.5 M TFA / 0.1 M HCl (in DI water)	-	14.4 ± 2.5	10 ⁴	OECT	
p(DPP _{BTEG} -TVT)			-	11 ± 2.4	10 ⁴	Bioelectronics	

OMIEC: Organic mixed ionic–electronic conductor; OECTs: organic electrochemical transistors; NR: natural rubber; PEDOT:PSS: poly(3,4-ethylenedioxythiophene):poly(styrenesulfonate); PBS: phosphate-buffered saline; MMT: montmorillonite; HA: hyaluronic acid; HEP: heparin; DS: dextran sulfate; CMCS: carboxymethyl chitosan; S-CNCs: sulfated-cellulose nanocrystal; LigS: lignosulfate; O3HT: oligo(3-hexylthiophene); PCL: polycaprolactone; TFA: trifluoroacetic acid; DI: deionized; HFIP: hexafluoroisopropanol; DPP: diketopyrrolopyrrole.

Partial degradation



Fully-acidic degradation

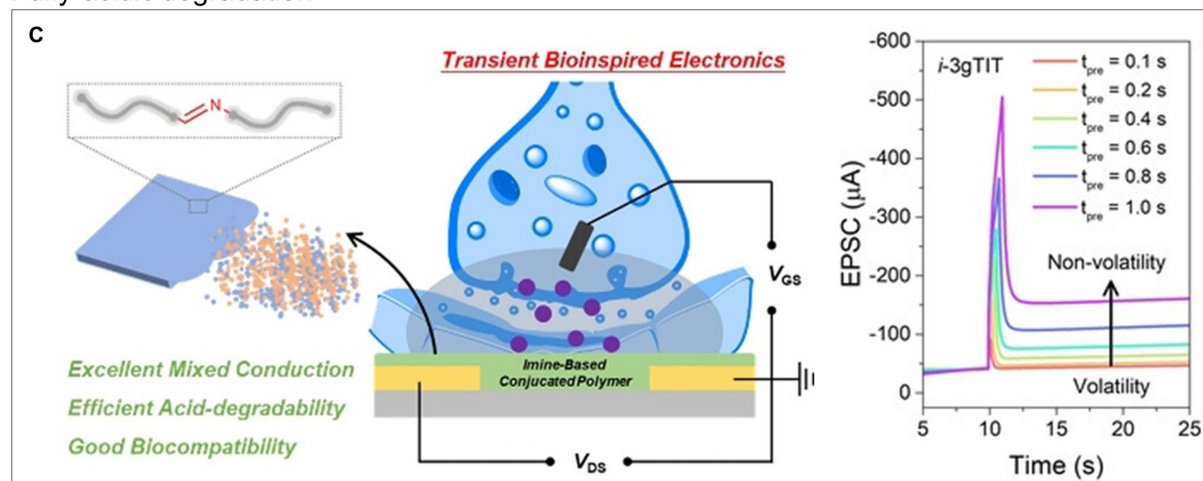


Figure 8. Biodegradable OMIECs for transient bioelectronics. (A) Left: Molecular structure of P(CL-co-AVL)-g-O3HT and optical photographs showing the biodegradation behavior of the P(CL-co-AVL)-LD-g-O3HT-30 films in water, 2 M TFA, and 2 M NaOH at 0, 3, and 7 days. Right: Drain current curves of the P(CL-co-AVL)-LD-g-O3HT-30-based OEET device before and after degradation in 2 M aqueous NaOH using PBS as the gate electrolyte and an Ag/AgCl gate electrode ($V_{ds} = 0$ – 0.8 V, $V_g = -0.6$ – 0.6 V). Reproduced with permission from Ref.^[37]. Copyright 2024, Royal Society of Chemistry; (B) Left: Molecular structure of PEDOT:Sacran, illustrating charge compensation between the positively charged PEDOT backbone and the negatively charged groups of Sacran. Right: Schematic representation of a flexible PET-based OEET employing PEDOT:Sacran as the channel material. Reproduced with permission from Ref.^[38] under the CC BY license; (C) Left: Schematic illustration of an OEET-based artificial synapse employing a fully biodegradable OMIEC as the channel material. The OMIEC contains acid-hydrolyzable imine linkages and yields biocompatible degradation products upon hydrolysis. Right: The graph illustrates spike-duration-dependent plasticity behavior of *i*-3gTIT devices induced by spike durations ranging from 0.1 to 1.0 s, exhibiting a clear transition from volatile to non-volatile memory states ($V_{GS,pre} = -1.5$ V, $V_{DS} = -0.5$ V). Reprinted with permission from Ref.^[46]. Copyright 2025, John Wiley & Sons. OMIECs: Organic mixed ionic–electronic conductors; O3HT: oligo(3-hexylthiophene); TFA: trifluoroacetic acid; OEET: organic electrochemical transistor; PBS: phosphate-buffered saline; PEDOT: poly(3,4-ethylenedioxythiophene); PET: poly(ethylene terephthalate); BOPLA: biaxially oriented poly(lactic acid); EPSC: excitatory postsynaptic current.

Table 8. Biodegradable natural polymer-based ionic conductors

Materials	Molecular weight (kDa)	Degree of functionalization (group name)
HA ^[41]	250-800	1 (carboxylic acid) ^[138]
Chondroitin sulfate ^[41]	20-30	1 (carboxylic acid) ^[139] 1-1.4 (sulfate)
HEP ^[40]	15-19	2.7 (sulfate, sulfonate)
DS ^[136]	500	1.35-1.85 (sulfate) ^[141]
CMCS ^[142]	400	1.1 (carboxymethyl acid)
S-CNCs ^[44]	-	0.06 (sulfate)
LigS ^[43]	52	0.7 (sulfonate)
Sacran ^[38]	2,350	0.1 (sulfate), 0.22 (carboxylic acid)

The degree of functionalization of HA, chondroitin sulfate and HEP was calculated based on the disaccharide unit. For other polymers, the values represent the number of functional groups per monosaccharide monomer. HA: Hyaluronic acid; HEP: heparin; DS: dextran sulfate; CMCS: carboxymethyl chitosan; S-CNCs: sulfated-cellulose nanocrystal; LigS: lignosulfate.

PET substrates [Figure 8B] showed stable operation and minimal performance variation under mechanical deformation. Devices fabricated on biodegradable PLA substrates achieved transconductance up to 1.6 mS and exhibited partial degradation in PBS and proteinase-containing environments^[38]. Although PEDOT:Sacran improves water stability and device performance^[38], the non-biodegradable PEDOT backbone remains a limitation.

The most advanced strategies incorporate degradable linkages directly into conjugated backbones. Representative examples include imine-linked systems such as *o*-3gTIT and *i*-3gTIT^[46], as well as related DPP-based polymers^[45] [Table 7]. These materials combine ionic compatibility from ethylene glycol side chains with programmed degradability from imine linkages^[45,46]. Regiochemical control in 3gTIT systems produced distinct packing structures, where *i*-3gTIT showed higher crystallinity and improved transconductance^[44]. These properties enabled OECTs, inverters, and artificial synapses [Figure 8C]. Devices exhibited stable excitatory and inhibitory postsynaptic currents (EPSC/IPSC), spike-timing-dependent plasticity, and tunable synaptic responses^[46]. Long retention times and operational stability enabled over 90% recognition accuracy in MNIST simulations^[46]. Degradation occurred through hydrolysis of imine bonds under acidic conditions, confirmed by molecular weight reduction and spectroscopic analysis^[46]. However, degradation behavior under physiological conditions remains unclear, and further optimization is required.

Overall, biodegradable OMIECs have evolved from composite-based systems to more advanced molecular designs that directly integrate degradability with OMIEC function. Further progress will require balancing degradation behavior, aqueous stability, and device performance.

CONCLUSION AND OUTLOOK

This review summarizes recent progress in biodegradable organic conductors, including conductive polymers, conductive composite pastes, and OMIECs, with a focus on material design strategies, degradation behavior, and device-level implementations. Across these material systems, a recurring challenge lies in balancing electrical performance, mechanical compliance, and controlled degradation. At the same time, the growing range of bioelectronic applications underscores the potential of these materials for minimally invasive, biointegrated systems.

Despite meaningful advances, several important challenges remain. First, achieving complete biodegradability under physiological conditions remains difficult, particularly for conjugated polymers and OMIECs. This challenge originates from the intrinsic stability of π -conjugated backbones, which conflicts

with the need for hydrolytically cleavable structures. Future work will require molecular designs that introduce degradable linkages while maintaining efficient charge transport. Such strategies will be essential for realizing fully bioresorbable organic electronic systems.

Second, the incorporation of degradable functionalities inherently introduces performance trade-offs compared to conventional non-degradable conductors. In general, biodegradable systems exhibit inferior electrical conductivity, mechanical stability, and long-term reliability. For example, hydrolytically cleavable moieties introduced into π -conjugated backbones can disrupt charge delocalization, leading to reduced conductivity. In composite pastes, premature disruption of percolation networks under aqueous conditions results in shortened functional lifetimes. In OMIECs, mismatches in the biodegradability of ionic and electronic components, along with incomplete degradation, further limit device stability. Addressing these challenges requires integrated material design strategies that simultaneously consider biodegradability, electrical performance, and long-term reliability.

Third, increasing demand for minimally invasive implantable systems and intelligent bioelectronics continues to drive higher levels of device integration. Accordingly, biodegradable organic conductors need to become compatible with scalable fabrication processes, including high-resolution patterning, multilayer integration, and system-level stability. Advances in both materials and processing will therefore be critical for enabling highly integrated transient bioelectronic platforms.

Beyond these material-level considerations, biodegradable organic conductors may also support broader system-level developments. The integration of sensing, actuation, and adaptive control within soft and deformable platforms points toward intelligent biodegradable systems, including soft robotic platforms and biointeractive devices. Such systems could operate in dynamic biological environments while maintaining mechanical compatibility and environmental sustainability. From a broader perspective, continued advances in biodegradable organic conductors may contribute to electronic systems that more closely resemble biological systems in both function and lifecycle. In this context, transient electronic platforms that ultimately degrade into environmentally benign byproducts, including compostable pathways, represent a meaningful direction for future research. These developments may extend transient bioelectronics beyond biomedical applications toward sustainable, human-compatible electronic systems.

DECLARATIONS

Acknowledgements

Graphical Abstract was created with BioRender (<https://BioRender.com>).

Authors' contributions

Outlined the manuscript structure: Choi, M. K.; Jeon, J. H.; Kim, Y. G.

Involved in the discussion: Choi, M. K.; Jeon, J. H.; Kim, Y. G.

Conducted the literature review and wrote the manuscript draft: Choi, M. K.; Jeon, J. H.; Kim, Y. G.

Supervised the manuscript: Kang, S. K.

Availability of data and materials

Not applicable.

AI and AI-assisted tools statement

During the preparation of this manuscript, the AI tool ChatGPT (version 5.4, released 2026-03-05) and Grammarly were used solely for language editing. These tools did not influence the study design, data collection, analysis, interpretation, or the scientific content of the work. All authors take full responsibility for the accuracy, integrity, and final content of the manuscript.

Financial support and sponsorship

This work was supported by the National Research Foundation of Korea (NRF) funded by the Ministry of Science and ICT (MSIT) (Grant No. RS-2025-25441247 and RS-2025-02305569).

Conflicts of interest

Kang, S. K. is the Guest Editor of the Special Topic “Transient and Biodegradable Soft Electronics and Robots for Sustainable and Biomedical Applications” in the *Soft Science*. Kang, S. K. had no involvement in the review or editorial process of this manuscript, including but not limited to reviewer selection, evaluation, or the final decision, while the other authors have declared that they have no conflicts.

Ethical approval and consent to participate

Not applicable.

Consent for publication

Not applicable.

Copyright

© The Author(s) 2026.

REFERENCES

1. Liu, Y.; Li, J.; Song, S.; et al. Morphing electronics enable neuromodulation in growing tissue. *Nat. Biotechnol.* **2020**, *38*, 1031-6. DOI PubMed PMC
2. Song, K. I.; Seo, H.; Seong, D.; et al. Adaptive self-healing electronic epineurium for chronic bidirectional neural interfaces. *Nat. Commun.* **2020**, *11*, 4195. DOI PubMed PMC
3. Frank, J. A.; Antonini, M. J.; Anikeeva, P. Next-generation interfaces for studying neural function. *Nat. Biotechnol.* **2019**, *37*, 1013-23. DOI PubMed PMC
4. Lacour, S. P.; Courtine, G.; Guck, J. Materials and technologies for soft implantable neuroprostheses. *Nat. Rev. Mater.* **2016**, *1*, 16063. DOI
5. Bettinger, C. J. Recent advances in materials and flexible electronics for peripheral nerve interfaces. *Bioelectron. Med.* **2018**, *4*, 6. DOI PubMed PMC
6. Weltman, A.; Yoo, J.; Meng, E. Flexible, penetrating brain probes enabled by advances in polymer microfabrication. *Micromachines* **2016**, *7*, 180. DOI PubMed PMC
7. Jeong, J. W.; Shin, G.; Park, S. I.; Yu, K. J.; Xu, L.; Rogers, J. A. Soft materials in neuroengineering for hard problems in neuroscience. *Neuron* **2015**, *86*, 175-86. DOI PubMed
8. Huang, Y.; Cui, Y.; Deng, H.; et al. Bioresorbable thin-film silicon diodes for the optoelectronic excitation and inhibition of neural activities. *Nat. Biomed. Eng.* **2023**, *7*, 486-98. DOI PubMed
9. Yu, K. J.; Kuzum, D.; Hwang, S. W.; et al. Bioresorbable silicon electronics for transient spatiotemporal mapping of electrical activity from the cerebral cortex. *Nat. Mater.* **2016**, *15*, 782-91. DOI PubMed PMC
10. Guo, L.; Ma, M.; Zhang, N.; Langer, R.; Anderson, D. G. Stretchable polymeric multielectrode array for conformal neural interfacing. *Adv. Mater.* **2014**, *26*, 1427-33. DOI PubMed PMC
11. Kim, J.; Yang, C.; Yun, T.; et al. Surface-embedding of Mo microparticles for robust and conductive biodegradable fiber electrodes: toward 1D flexible transient electronics. *Adv. Sci.* **2023**, *10*, e2206186. DOI PubMed PMC
12. Kim, J.; Jeon, J.; Lee, J. Y.; et al. Electroceuticals for regeneration of long nerve gap using biodegradable conductive conduits and implantable wireless stimulator. *Adv. Sci.* **2023**, *10*, e2302632. DOI PubMed PMC
13. Rivers, T. J.; Hudson, T. W.; Schmidt, C. E. Synthesis of a novel, biodegradable electrically conducting polymer for biomedical applications. *Adv. Funct. Mater.* **2002**, *12*, 33-7. DOI
14. Wang, Z.; Roberge, C.; Wan, Y.; Dao, L. H.; Guidoin, R.; Zhang, Z. A biodegradable electrical bioconductor made of polypyrrole nanoparticle/poly(D,L-lactide) composite: a preliminary in vitro biostability study. *J. Biomed. Mater. Res. A.* **2003**, *66*, 738-46. DOI PubMed
15. Shi, G.; Rouabhia, M.; Wang, Z.; Dao, L. H.; Zhang, Z. A novel electrically conductive and biodegradable composite made of polypyrrole nanoparticles and polylactide. *Biomaterials* **2004**, *25*, 2477-88. DOI PubMed
16. Shahdan, D.; Chen, R. S.; Ahmad, S.; Zailan, F. D.; Mat Ali, A. Assessment of mechanical performance, thermal stability and water resistance of novel conductive poly(lactic acid)/modified natural rubber blends with low loading of polyaniline. *Polym. Int.* **2018**, *67*, 1070-80. DOI

17. Guo, B.; Finne-Wistrand, A.; Albertsson, A. Degradable and electroactive hydrogels with tunable electrical conductivity and swelling behavior. *Chem. Mater.* **2011**, *23*, 1254-62. [DOI](#)
18. Chen, J.; Yu, M.; Guo, B.; Ma, P. X.; Yin, Z. Conductive nanofibrous composite scaffolds based on in-situ formed polyaniline nanoparticle and polylactide for bone regeneration. *J. Colloid. Interface. Sci.* **2018**, *514*, 517-27. [DOI PubMed](#)
19. Shafei, S.; Foroughi, J.; Stevens, L.; Wong, C. S.; Zabihi, O.; Naebe, M. Electroactive nanostructured scaffold produced by controlled deposition of PPy on electrospun PCL fibres. *Res. Chem. Intermed.* **2017**, *43*, 1235-51. [DOI](#)
20. Sarvari, R.; Akbari-Alanjaraghi, M.; Massoumi, B.; Beygi-Khosrowshahi, Y.; Agbolaghi, S. Conductive and biodegradable scaffolds based on a five-arm and functionalized star-like polyaniline–polycaprolactone copolymer with a D-glucose core. *New. J. Chem.* **2017**, *41*, 6371-84. [DOI](#)
21. Guex, A. G.; Spicer, C. D.; Armgarth, A.; et al. Electrospun aniline-tetramer-co-polycaprolactone fibres for conductive, biodegradable scaffolds. *MRS. Commun.* **2017**, *7*, 375-82. [DOI PubMed PMC](#)
22. Cabuk, M.; Alan, Y.; Yavuz, M.; Unal, H. I. Synthesis, characterization and antimicrobial activity of biodegradable conducting polypyrrole-graft-chitosan copolymer. *Appl. Surf. Sci.* **2014**, *318*, 168-75. [DOI](#)
23. Zhang, Q. S.; Yan, Y. H.; Li, S. P.; Feng, T. Synthesis of a novel biodegradable and electroactive polyphosphazene for biomedical application. *Biomed. Mater.* **2009**, *4*, 035008. [DOI PubMed](#)
24. Cui, H.; Liu, Y.; Deng, M.; et al. Synthesis of biodegradable and electroactive tetraaniline grafted poly(ester amide) copolymers for bone tissue engineering. *Biomacromolecules* **2012**, *13*, 2881-9. [DOI PubMed](#)
25. Domagala, A.; Maksymiak, M.; Janeczek, H.; et al. Oligo-3-hydroxybutyrate functionalised pyrroles for preparation of biodegradable conductive polymers. *J. Mater. Sci.* **2014**, *49*, 5227-36. [DOI](#)
26. Guo, B.; Qu, J.; Zhao, X.; Zhang, M. Degradable conductive self-healing hydrogels based on dextran-graft-tetraaniline and N-carboxyethyl chitosan as injectable carriers for myoblast cell therapy and muscle regeneration. *Acta. Biomater.* **2019**, *84*, 180-93. [DOI PubMed](#)
27. Shi, M.; Dong, R.; Hu, J.; Guo, B. Conductive self-healing biodegradable hydrogel based on hyaluronic acid-grafted-polyaniline as cell recruitment niches and cell delivery carrier for myogenic differentiation and skeletal muscle regeneration. *Chem. Eng. J.* **2023**, *457*, 141110. [DOI](#)
28. Hardy, J. G.; Mouser, D. J.; Arroyo-Currás, N.; et al. Biodegradable electroactive polymers for electrochemically-triggered drug delivery. *J. Mater. Chem. B.* **2014**, *2*, 6809-22. [DOI](#)
29. Lee, S.; Hong, Y.; Shim, B. S. Biodegradable PEDOT:PSS/clay composites for multifunctional green-electronic materials. *Adv. Sustain. Syst.* **2022**, *6*, 2100056. [DOI](#)
30. Xu, C.; Yopez, G.; Wei, Z.; Liu, F.; Bugarin, A.; Hong, Y. Synthesis and characterization of conductive, biodegradable, elastomeric polyurethanes for biomedical applications. *J. Biomed. Mater. Res. A.* **2016**, *104*, 2305-14. [DOI PubMed PMC](#)
31. Lei, T.; Guan, M.; Liu, J.; et al. Biocompatible and totally disintegrable semiconducting polymer for ultrathin and ultralightweight transient electronics. *Proc. Natl. Acad. Sci. U. S. A.* **2017**, *114*, 5107-12. [DOI PubMed PMC](#)
32. Atreya, M.; Dikshit, K.; Marinick, G.; Nielson, J.; Bruns, C.; Whiting, G. L. Poly(lactic acid)-based ink for biodegradable printed electronics with conductivity enhanced through solvent aging. *ACS. Appl. Mater. Interfaces.* **2020**, *12*, 23494-501. [DOI PubMed](#)
33. Kim, K.; Yoo, J.; Shim, J.; et al. Biodegradable molybdenum/polybutylene adipate terephthalate conductive paste for flexible and stretchable transient electronics. *Adv. Mater. Technol.* **2022**, *7*, 2001297. [DOI](#)
34. Chae, J. W.; Lee, D.; Osman, A.; et al. Silk fibroin, sericin, and conductive silk composites for skin-attachable transient electronics. *ACS. Appl. Electron. Mater.* **2024**, *6*, 1746-56. [DOI](#)
35. Kim, K. S.; Maeng, W. Y.; Kim, S.; et al. Isotropic conductive paste for bioresorbable electronics. *Mater. Today. Bio.* **2023**, *18*, 100541. [DOI PubMed PMC](#)
36. Paulsen, B. D.; Tybrandt, K.; Stavrinidou, E.; Rivnay, J. Organic mixed ionic-electronic conductors. *Nat. Mater.* **2020**, *19*, 13-26. [DOI PubMed](#)
37. Lee, Y.; Yim, S. G.; Lee, G. W.; et al. Self-adherent biodegradable gelatin-based hydrogel electrodes for electrocardiography monitoring. *Sensors* **2020**, *20*, 5737. [DOI PubMed PMC](#)
38. Matura, K.; Putz, C.; Hradilova, S.; et al. Algal polysaccharide Sacran-based conductive nanocomposites for ultrathin flexible and biodegradable organic electrochemical transistors. *Npj. Flex. Electron.* **2025**, *9*, 56. [DOI PubMed PMC](#)
39. Xu, C.; Guan, S.; Wang, S.; et al. Biodegradable and electroconductive poly(3,4-ethylenedioxythiophene)/carboxymethyl chitosan hydrogels for neural tissue engineering. *Mater. Sci. Eng. C. Mater. Biol. Appl.* **2018**, *84*, 32-43. [DOI PubMed](#)
40. Pal, R. K.; Farghaly, A. A.; Wang, C.; Collinson, M. M.; Kundu, S. C.; Yadavalli, V. K. Conducting polymer-silk biocomposites for flexible and biodegradable electrochemical sensors. *Biosens. Bioelectron.* **2016**, *81*, 294-302. [DOI PubMed](#)
41. Mantione, D.; Del Agua, I.; Schaafsma, W.; et al. Poly(3,4-ethylenedioxythiophene):glycosaminoglycan aqueous dispersions: toward electrically conductive bioactive materials for neural interfaces. *Macromol. Biosci.* **2016**, *16*, 1227-38. [DOI PubMed](#)

42. Ner, Y.; Invernale, M. A.; Grote, J. G.; Stuart, J. A.; Sotzing, G. A. Facile chemical synthesis of DNA-doped PEDOT. *Synth. Met.* **2010**, *160*, 351-3. DOI
43. Matura, K.; Grabner, T.; Hradilova, S.; et al. Wood-based bioelectronics: lignosulfonate-based conductive biocomposites for paper organic electrochemical transistors. *Adv. Elect. Mater.* **2026**, e00809. DOI
44. Matura, K.; D'Orsi, R.; Spagnuolo, L.; et al. Nanocrystalline cellulose-based mixed ionic–electronic conductor for bioelectronics. *J. Mater. Chem. C* **2024**, *12*, 16701-13. DOI
45. Lin, A.; Liu, Z.; Upreti, S.; et al. Degradable donor-acceptor polymeric mixed ionic-electronic conductors for transient electronics. *Adv. Mater. Technol.* **2026**, *11*, e02543. DOI
46. Chen, J.; Cong, S.; Liu, R.; et al. Imine-based polymeric mixed ionic-electronic conductors featuring degradability and biocompatibility for transient bioinspired electronics. *Angew. Chem. Int. Ed. Engl.* **2025**, *64*, e202417921. DOI PubMed
47. Feig, V. R.; Tran, H.; Bao, Z. Biodegradable polymeric materials in degradable electronic devices. *ACS. Cent. Sci.* **2018**, *4*, 337-48. DOI PubMed PMC
48. Root, S. E.; Savagatrup, S.; Printz, A. D.; Rodriguez, D.; Lipomi, D. J. Mechanical properties of organic semiconductors for stretchable, highly flexible, and mechanically robust electronics. *Chem. Rev.* **2017**, *117*, 6467-99. DOI PubMed
49. Nezakati, T.; Seifalian, A.; Tan, A.; Seifalian, A. M. Conductive polymers: opportunities and challenges in biomedical applications. *Chem. Rev.* **2018**, *118*, 6766-843. DOI PubMed
50. Wang, J.; Cao, J.; Xu, Y.; An, H.; Li, X. Fabrication of a flexible porous polypyrrole film with a 3D micro-nanostructure and its electrochemical properties. *Phys. Chem. Chem. Phys.* **2023**, *25*, 10925-34. DOI
51. Eom, T.; Lee, J.; Lee, S.; et al. Highly conductive polydopamine coatings by direct electrochemical synthesis on Au. *ACS. Appl. Polym. Mater.* **2022**, *4*, 5319-29. DOI
52. Szweczyk, J.; Aguilar-Ferrer, D.; Coy, E. Polydopamine films: electrochemical growth and sensing applications. *Eur. Polym. J.* **2022**, *174*, 111346. DOI
53. Bettinger, C. J.; Bruggeman, J. P.; Misra, A.; Borenstein, J. T.; Langer, R. Biocompatibility of biodegradable semiconducting melanin films for nerve tissue engineering. *Biomaterials* **2009**, *30*, 3050-7. DOI PubMed PMC
54. Zanzanjadeh Ezazi, N.; Ajdary, R.; Correia, A.; et al. Fabrication and characterization of drug-loaded conductive poly(glycerol sebacate)/nanoparticle-based composite patch for myocardial infarction applications. *ACS. Appl. Mater. Interfaces.* **2020**, *12*, 6899-909. DOI PubMed PMC
55. Imam, S. H.; Gordon, S. H.; Shogren, R. L.; Tosteson, T. R.; Govind, N. S.; Greene, R. V. Degradation of starch-poly(beta-hydroxybutyrate-co-beta-hydroxyvalerate) bioplastic in tropical coastal waters. *Appl. Environ. Microbiol.* **1999**, *65*, 431-7. DOI PubMed PMC
56. Vikhoreva, G. A.; Kil'deeva, N. R.; Ustinov, M. Y.; Nochevkina, Y. N. Fabrication and study of the degradability of chitosan films. *Fibre. Chem.* **2002**, *34*, 407-11. DOI
57. Tomihata, K.; Ikada, Y. In vitro and in vivo degradation of films of chitin and its deacetylated derivatives. *Biomaterials* **1997**, *18*, 567-75. DOI PubMed
58. Bose, S.; Li, S.; Mele, E.; Williams, C. J.; Silberschmidt, V. V. Stability and mechanical performance of collagen films under different environmental conditions. *Polym. Degrad. Stab.* **2022**, *197*, 109853. DOI
59. Wang, Y.; Mo, W.; Yao, H.; Wu, Q.; Chen, J.; Chen, G. Biodegradation studies of poly(3-hydroxybutyrate-co-3-hydroxyhexanoate). *Polym. Degrad. Stab.* **2004**, *85*, 815-21. DOI
60. Barajas-Ledesma, R. M.; Stocker, C. W.; Wong, V. N.; Little, K.; Patti, A. F.; Garnier, G. Biodegradation of a nanocellulose superabsorbent and its effect on the growth of spinach (*Spinacea oleracea*). *ACS. Agric. Sci. Technol.* **2022**, *2*, 90-9. DOI
61. Li, C.; Meng, X.; Gong, W.; Chen, S.; Wen, W.; Xin, Z. Hydrolytic aging of degradable poly(glycolic acid) at different temperatures. *Ind. Eng. Chem. Res.* **2024**, *63*, 1864-74. DOI
62. Ogueri, K. S.; Escobar Ivirico, J. L.; Nair, L. S.; Allcock, H. R.; Laurencin, C. T. Biodegradable polyphosphazene-based blends for regenerative engineering. *Regen. Eng. Transl. Med.* **2017**, *3*, 15-31. DOI PubMed PMC
63. Nazarzadeh Zareh, E.; Najafi Moghadam, P.; Azariyan, E.; Sharifian, I. Conductive and biodegradable polyaniline/starch blends and their composites with polystyrene. *Iran. Polym. J.* **2011**, *20*, 319-28. <https://www.sid.ir/FileServer/JE/813201113005>. (accessed 2026-06-10).
64. Nazarzadeh Zare, E.; Mansour Lakouraj, M.; Mohseni, M. Biodegradable polypyrrole/dextrin conductive nanocomposite: synthesis, characterization, antioxidant and antibacterial activity. *Synth. Met.* **2014**, *187*, 9-16. DOI
65. Gu, B. K.; Kim, M. S.; Kang, C. M.; Kim, J. L.; Park, S. J.; Kim, C. H. Fabrication of conductive polymer-based nanofiber scaffolds for tissue engineering applications. *J. Nanosci. Nanotechnol.* **2014**, *14*, 7621-6. DOI PubMed
66. Liu, Y.; Peng, X.; Ye, H.; Xu, J.; Chen, F. Fabrication and properties of conductive chitosan/polypyrrole composite fibers. *Polym. Plast. Technol. Eng.* **2015**, *54*, 411-5. DOI

-
67. Liu, D.; Huyan, C.; Wang, Z.; et al. Conductive polymer based hydrogels and their application in wearable sensors: a review. *Mater. Horiz.* **2023**, *10*, 2800-23. DOI PubMed
 68. Thongruang, W.; Spontak, R. J.; Balik, C. Correlated electrical conductivity and mechanical property analysis of high-density polyethylene filled with graphite and carbon fiber. *Polymer* **2002**, *43*, 2279-86. DOI
 69. Jin, J.; Lin, Y.; Song, M.; Gui, C.; Leesirisan, S. Enhancing the electrical conductivity of polymer composites. *Eur. Polym. J.* **2013**, *49*, 1066-72. DOI
 70. Lay, M.; Méndez, J. A.; Delgado-Aguilar, M.; Bun, K. N.; Vilaseca, F. Strong and electrically conductive nanopaper from cellulose nanofibers and polypyrrole. *Carbohydr. Polym.* **2016**, *152*, 361-9. DOI PubMed
 71. Han, J.; Lu, K.; Yue, Y.; et al. Nanocellulose-templated assembly of polyaniline in natural rubber-based hybrid elastomers toward flexible electronic conductors. *Ind. Crops. Prod.* **2019**, *128*, 94-107. DOI
 72. Vijayavenkataraman, S.; Kannan, S.; Cao, T.; Fuh, J. Y. H.; Sriram, G.; Lu, W. F. 3D-printed PCL/PPy conductive scaffolds as three-dimensional porous nerve guide conduits (NGCs) for peripheral nerve injury repair. *Front. Bioeng. Biotechnol.* **2019**, *7*, 266. DOI PubMed PMC
 73. Sun, X.; Chan, E. W. C.; Chen, Q.; et al. Copolymers of gelatin-graft-poly(3-hexylthiophene) for transient electronics. *ACS. Appl. Mater. Interfaces.* **2024**, *16*, 23872-84. DOI PubMed
 74. Nepomuceno, N.; Seixas, A.; Medeiros, E.; Mélo, T. Evaluation of conductivity of nanostructured polyaniline/cellulose nanocrystals (PANI/CNC) obtained via in situ polymerization. *J. Solid. State. Chem.* **2021**, *302*, 122372. DOI
 75. Nur Hidayah, S.; Dania Adila, A. R.; Sharaniza, A. R.; Muhammad Abid, A.; Mohd Muzamir, M. Sequentially crosslinked collagen-based hydrogel to form a semi-interpenetrating network for enhanced stability to hydrolytic degradation and electrochemical properties. *Polym. Adv. Technol.* **2024**, *35*, e6546. DOI
 76. Durgam, H.; Sapp, S.; Deister, C.; et al. Novel degradable co-polymers of polypyrrole support cell proliferation and enhance neurite out-growth with electrical stimulation. *J. Biomater. Sci. Polym. Ed.* **2010**, *21*, 1265-82. DOI PubMed PMC
 77. Massoumi, B.; Sarvari, R.; Agbolaghi, S. Biodegradable and conductive hyperbranched terpolymers based on aliphatic polyester, poly(D, L-lactide), and polyaniline used as scaffold in tissue engineering. *Int. J. Polym. Mater. Polym. Biomater.* **2018**, *67*, 808-21. DOI
 78. Jo, G.; Kim, O.; Kim, H.; Hyeok Choi, U.; Lee, S.; Jeong Park, M. End-functionalized block copolymer electrolytes: effect of segregation strength on ion transport efficiency. *Polym. J.* **2016**, *48*, 465-72. DOI
 79. Dominguez-Alfaro, A.; Criado-Gonzalez, M.; Gaborondo, E.; et al. Electroactive 3D printable poly(3,4-ethylenedioxythiophene)-graft-poly(ϵ -caprolactone) copolymers as scaffolds for muscle cell alignment. *Polym. Chem.* **2021**, *13*, 109-20. DOI
 80. Da Silva, A. C.; Paschoal, V. H.; Ribeiro, M. C. C.; de Torresi, S. I. C. Electrical/spectroscopic stability of conducting and biodegradable graft-copolymer. *Macromol. Chem. Phys.* **2022**, *223*, 2200275. DOI
 81. Sun, X.; Barker, D.; Travas-Sejdic, J. Transient degradable electronics enabled by systems of conducting polymers and natural biopolymers. *J. Mater. Chem. C.* **2026**, *14*, 4228-47. DOI
 82. Maia, M.; Nunes, F. M. Authentication of beeswax (*Apis mellifera*) by high-temperature gas chromatography and chemometric analysis. *Food. Chem.* **2013**, *136*, 961-8. DOI PubMed
 83. Srisakvarangkool, W.; Chanthasena, P.; Rosyidah, A.; Ganta, P.; Kerdtob, S.; Nantapong, N. Biodegradation of plastic waste by yellow mealworms (*Tenebrio molitor* larvae). *PeerJ* **2026**, *14*, e20429. DOI PubMed PMC
 84. Jin, L.; Feng, P.; Cheng, Z.; Wang, D. Effect of biodegrading polyethylene, polystyrene, and polyvinyl chloride on the growth and development of yellow mealworm (*Tenebrio molitor*) larvae. *Environ. Sci. Pollut. Res. Int.* **2023**, *30*, 37118-26. DOI PubMed
 85. Eom, T.; Jeon, J.; Lee, S.; et al. Naturally derived melanin nanoparticle composites with high electrical conductivity and biodegradability. *Part. Part. Syst. Character.* **2019**, *36*, 1900166. DOI
 86. Guo, B.; Finne-Wistrand, A.; Albertsson, A. Enhanced electrical conductivity by macromolecular architecture: hyperbranched electroactive and degradable block copolymers based on poly(ϵ -caprolactone) and aniline pentamer. *Macromolecules* **2010**, *43*, 4472-80. DOI
 87. Baheiraei, N.; Gharibi, R.; Yeganeh, H.; et al. Electroactive polyurethane/siloxane derived from castor oil as a versatile cardiac patch, part I: Synthesis, characterization, and myoblast proliferation and differentiation. *J. Biomed. Mater. Res. A.* **2016**, *104*, 775-87. DOI
 88. Wu, Y.; Wang, L.; Guo, B.; Shao, Y.; Ma, P. X. Electroactive biodegradable polyurethane significantly enhanced Schwann cells myelin gene expression and neurotrophin secretion for peripheral nerve tissue engineering. *Biomaterials* **2016**, *87*, 18-31. DOI PubMed
 89. Xu, C.; Huang, Y.; Yezep, G.; et al. Development of dopant-free conductive bioelastomers. *Sci. Rep.* **2016**, *6*, 34451. DOI PubMed PMC
 90. Zhang, Y.; Tang, J.; Fang, W.; et al. Synergetic effect of electrical and topographical cues in aniline trimer-based polyurethane fibrous scaffolds on tissue regeneration. *J. Funct. Biomater.* **2023**, *14*, 185. DOI PubMed PMC
 91. Place, E. S.; Evans, N. D.; Stevens, M. M. Complexity in biomaterials for tissue engineering. *Nat. Mater.* **2009**, *8*, 457-70. DOI PubMed

-
92. Balint, R.; Cassidy, N. J.; Cartmell, S. H. Conductive polymers: towards a smart biomaterial for tissue engineering. *Acta. Biomater.* **2014**, *10*, 2341-53. DOI PubMed
 93. Hardy, J. G.; Lee, J. Y.; Schmidt, C. E. Biomimetic conducting polymer-based tissue scaffolds. *Curr. Opin. Biotechnol.* **2013**, *24*, 847-54. DOI PubMed
 94. Liu, Y.; Cui, H.; Zhuang, X.; Wei, Y.; Chen, X. Electrospinning of aniline pentamer-graft-gelatin/PLLA nanofibers for bone tissue engineering. *Acta. Biomater.* **2014**, *10*, 5074-80. DOI PubMed
 95. Chiong, J. A.; Zheng, Y.; Zhang, S.; et al. Impact of molecular design on degradation lifetimes of degradable imine-based semiconducting polymers. *J. Am. Chem. Soc.* **2022**, *144*, 3717-26. DOI
 96. Sugiyama, F.; Kleinschmidt, A. T.; Kayser, L. V.; et al. Stretchable and degradable semiconducting block copolymers. *Macromolecules* **2018**, *51*, 5944-9. DOI PubMed PMC
 97. Wang, Y.; Wu, C.; Zhang, Y.; Du, S.; Zhou, X. Wearable and implantable transient bioelectronics. *J. Mater. Chem. C.* **2025**, *13*, 14682-96. DOI
 98. Liu, Z.; Wei, W.; Tremblay, P. L.; Zhang, T. Electrostimulation of fibroblast proliferation by an electrospun poly (lactide-co-glycolide)/polydopamine/chitosan membrane in a humid environment. *Colloids. Surf. B. Biointerfaces.* **2022**, *220*, 112902. DOI
 99. Qu, J.; Liang, Y.; Shi, M.; Guo, B.; Gao, Y.; Yin, Z. Biocompatible conductive hydrogels based on dextran and aniline trimer as electro-responsive drug delivery system for localized drug release. *Int. J. Biol. Macromol.* **2019**, *140*, 255-64. DOI PubMed
 100. Bagheri, B.; Zarrintaj, P.; Surwase, S. S.; et al. Self-gelling electroactive hydrogels based on chitosan-aniline oligomers/agarose for neural tissue engineering with on-demand drug release. *Colloids. Surf. B. Biointerfaces.* **2019**, *184*, 110549. DOI PubMed
 101. Zhou, L.; Zheng, H.; Wang, S.; Zhou, F.; Lei, B.; Zhang, Q. Biodegradable conductive multifunctional branched poly(glycerol-amino acid)-based scaffolds for tumor/infection-impaired skin multimodal therapy. *Biomaterials* **2020**, *262*, 120300. DOI PubMed
 102. Tran, H.; Feig, V. R.; Liu, K.; et al. Stretchable and fully degradable semiconductors for transient electronics. *ACS. Cent. Sci.* **2019**, *5*, 1884-91. DOI PubMed PMC
 103. Chen, C.; Bai, X.; Ding, Y.; Lee, I. S. Electrical stimulation as a novel tool for regulating cell behavior in tissue engineering. *Biomater. Res.* **2019**, *23*, 25. DOI PubMed PMC
 104. Raval, A.; Parikh, J.; Engineer, C. Mechanism and in vitro release kinetic study of sirolimus from a biodegradable polymeric matrix coated cardiovascular stent. *Ind. Eng. Chem. Res.* **2011**, *50*, 9539-49. DOI
 105. Zhou, N.; Zhang, L.; Cui, T.; Wu, P.; Lei, Z. Design and applications of conductive polymers in wearable electrophysiological sensing. *Sci. China. Technol. Sci.* **2025**, *68*, 3114. DOI
 106. Lee, D. H.; Park, T.; Yoo, H. Biodegradable polymer composites for electrophysiological signal sensing. *Polymers* **2022**, *14*, 2875. DOI PubMed PMC
 107. Irimia-Vladu, M.; Troshin, P. A.; Reisinger, M.; et al. Biocompatible and biodegradable materials for organic field-effect transistors. *Adv. Funct. Mater.* **2010**, *20*, 4069-76. DOI
 108. Kim, Y.; Kim, K.; Park, J.; Lee, W.; Bae, J.; Kang, S. Fully biodegradable and mass-producible conductive fiber based on tungsten-poly(butylene adipate-co-terephthalate) composite. *npj. Flex. Electron.* **2025**, *9*, 448. DOI
 109. Aydemir, Sezer, U.; Ozturk Yavuz, K.; Ors, G.; et al. Zero-valent iron nanoparticles containing nanofiber scaffolds for nerve tissue engineering. *J. Tissue. Eng. Regen. Med.* **2020**, *14*, 1815-26. DOI PubMed
 110. Tan, M. A.; Yeoh, C. K.; Teh, P. L.; Abdul Rahim, N. A.; Song, C. C.; Mansor, N. S. S. Effect of combination printing parameter (infill density and raster angle) on the mechanical and electrical properties of 3D printed PLA/ZnO and cPLA/ZnO composites. *J. Polym. Eng.* **2022**, *42*, 351-61. DOI
 111. Lee, S.; Koo, J.; Kang, S.; et al. Metal microparticle - polymer composites as printable, bio/ecoresorbable conductive inks. *Mater. Today.* **2018**, *21*, 207-15. DOI
 112. Wei, Z.; Ma, X.; Zhao, H.; Wu, X.; Guo, Q. Accelerable self-sintering of solvent-free molybdenum/wax biodegradable composites for multimodally transient electronics. *ACS. Appl. Mater. Interfaces.* **2022**, *14*, 33472-81. DOI PubMed
 113. Aydemir Sezer, U.; Ozturk, K.; Aru, B.; Yanıkaya Demirel, G.; Sezer, S.; Bozkurt, M. R. Zero valent zinc nanoparticles promote neuroglial cell proliferation: a biodegradable and conductive filler candidate for nerve regeneration. *J. Mater. Sci. Mater. Med.* **2017**, *28*, 19. DOI PubMed
 114. Zhang, T.; Tsang, M.; Du, L.; Kim, M.; Allen, M. G. Electrical interconnects fabricated from biodegradable conductive polymer composites. *IEEE. Trans. Compon. Packaging. Manuf. Technol.* **2019**, *9*, 822-9. DOI PubMed PMC
 115. Mamunya, E. P.; Davidenko, V. V.; Lebedev, E. V. Percolation conductivity of polymer composites filled with dispersed conductive filler. *Polym. Compos.* **1995**, *16*, 319-24. DOI
 116. Babinec, S. J.; Mussell, R. D.; Lundgard, R. L.; Cieslinski, R. Electroactive thermoplastics. *Adv. Mater.* **2000**, *12*, 1823-34. DOI
 117. Yin, L.; Cheng, H.; Mao, S.; et al. Dissolvable metals for transient electronics. *Adv. Funct. Mater.* **2014**, *24*, 645-58. DOI

118. Choi, Y. S.; Koo, J.; Lee, Y. J.; et al. Biodegradable polyanhydrides as encapsulation layers for transient electronics. *Adv. Funct. Mater.* **2020**, *30*, 2000941. DOI
119. Lyu, J. S.; Lee, J. S.; Han, J. Development of a biodegradable polycaprolactone film incorporated with an antimicrobial agent via an extrusion process. *Sci. Rep.* **2019**, *9*, 20236. DOI PubMed PMC
120. Guo, Z.; Bo, D.; He, Y.; Luo, X.; Li, H. Degradation properties of chitosan microspheres/poly(L-lactic acid) composite in vitro and in vivo. *Carbohydr. Polym.* **2018**, *193*, 1-8. DOI PubMed
121. Vey, E.; Rodger, C.; Booth, J.; Claybourn, M.; Miller, A. F.; Saiani, A. Degradation kinetics of poly(lactic-co-glycolic) acid block copolymer cast films in phosphate buffer solution as revealed by infrared and Raman spectroscopies. *Polym. Degrad. Stab.* **2011**, *96*, 1882-9. DOI
122. Xu, J.; Feng, K.; Li, Y.; et al. Enhanced biodegradation rate of poly(butylene adipate-co-terephthalate) composites using reed fiber. *Polymers* **2024**, *16*, 411. DOI PubMed PMC
123. Kończak, B.; Uszok, E.; Białowas, M.; et al. Biodegradation of hydrophobic coatings based on natural wax and its mixtures. *Sustainability* **2026**, *18*, 509. DOI
124. Beena, M.; Ameer, J. M.; Kasoju, N. Optically clear silk fibroin films with tunable properties for potential corneal tissue engineering applications: a process-property-function relationship study. *ACS. Omega.* **2022**, *7*, 29634-46. DOI PubMed PMC
125. Li, C.; Guo, C.; Fitzpatrick, V.; et al. Design of biodegradable, implantable devices towards clinical translation. *Nat. Rev. Mater.* **2020**, *5*, 61-81. DOI
126. Xue, T.; Song, D.; Liu, Q.; Yu, J.; Wang, J. Dual-function conductive silver paste: application of an epoxy system based on curing resistance evolution in packaging and flexible electronics. *J. Mater. Chem. C.* **2026**, *14*, 5411-22. DOI
127. Kim, T. G.; Eom, H. S.; Kim, J. H.; Jung, J. K.; Jang, K. S.; Lee, S. J. Electrically conductive silicone-based nanocomposites incorporated with carbon nanotubes and silver nanowires for stretchable electrodes. *ACS. Omega.* **2021**, *6*, 31876-90. DOI PubMed PMC
128. Qiao, W.; Bao, H.; Li, X.; Jin, S.; Gu, Z. Research on electrical conductive adhesives filled with mixed filler. *Int. J. Adhes. Adhes.* **2014**, *48*, 159-63. DOI
129. Yang, Q.; Lee, S.; Xue, Y.; et al. Materials, mechanics designs, and bioresorbable multisensor platforms for pressure monitoring in the intracranial space. *Adv. Funct. Mater.* **2020**, *30*, 1910718. DOI
130. Choi, Y. S.; Yin, R. T.; Pfenniger, A.; et al. Fully implantable and bioresorbable cardiac pacemakers without leads or batteries. *Nat. Biotechnol.* **2021**, *39*, 1228-38. DOI PubMed PMC
131. Kim, K.; Shim, J.; Kim, S.; et al. Biodegradable yet hyperdurable robotic fingers for zero-waste soft electronics. *Nat. Sustain.* **2026**, *9*, 692-705. DOI
132. Rivnay, J.; Inal, S.; Salleo, A.; Owens, R. M.; Berggren, M.; Malliaras, G. G. Organic electrochemical transistors. *Nat. Rev. Mater.* **2018**, *3*, 17086. DOI
133. Gao, R.; Chen, W.; Zhang, X.; Chen, X.; Lu, C. Sensing-actuation system with zero signal delay for ultrasensitive recognition. *Mater. Today.* **2025**, *88*, 338-47. DOI
134. Nozella, N. L.; Lima, J. V. M.; de Oliveira, R. F.; Graeff, C. F. D. O. Melanin/PEDOT:PSS blend as organic mixed ionic electronic conductor (OMIEC) for sustainable electronics. *Mater. Adv.* **2023**, *4*, 4732-43. DOI
135. Hachim, D.; Hernández-Cruz, O.; Foote, J. E. J.; et al. Self-doped and biodegradable glycosaminoglycan-PEDOT conductive hydrogels facilitate electrical pacing of iPSC-derived cardiomyocytes. *Adv. Healthc. Mater.* **2025**, *14*, e2403995. DOI PubMed PMC
136. Harman, D. G.; Gorkin, R. 3rd.; Stevens, L.; et al. Poly(3,4-ethylenedioxythiophene):dextran sulfate (PEDOT:DS) - a highly processable conductive organic biopolymer. *Acta. Biomater.* **2015**, *14*, 33-42. DOI PubMed
137. Chan, E. W. C.; Sun, X.; Uda, Y.; Zhu, B.; Barker, D.; Travas-Sejdic, J. Transient polymer electronics enabled by grafting of oligo-3-hexylthiophenes onto polycaprolactone. *J. Mater. Chem. C.* **2024**, *12*, 11157-73. DOI
138. Bokaty, A. N.; Dubashynskaya, N. V.; Skorik, Y. A. Chemical modification of hyaluronic acid as a strategy for the development of advanced drug delivery systems. *Carbohydr. Polym.* **2024**, *337*, 122145. DOI PubMed
139. Shen, Q.; Guo, Y.; Wang, K.; Zhang, C.; Ma, Y. A review of chondroitin sulfate's preparation, properties, functions, and applications. *Molecules* **2023**, *28*, 7093. DOI PubMed PMC
140. Paluck, S. J.; Nguyen, T. H.; Maynard, H. D. Heparin-mimicking polymers: synthesis and biological applications. *Biomacromolecules* **2016**, *17*, 3417-40. DOI PubMed PMC
141. Madkhali, O. A.; Sivagurunathan Moni, S.; Sultan, M. H.; et al. Formulation and evaluation of injectable dextran sulfate sodium nanoparticles as a potent antibacterial agent. *Sci. Rep.* **2021**, *11*, 9914. DOI PubMed PMC
142. Chen, X.; Park, H. Chemical characteristics of O-carboxymethyl chitosans related to the preparation conditions. *Carbohydr. Polym.* **2003**, *53*, 355-9. DOI
143. Crouzier, T.; Boudou, T.; Picart, C. Polysaccharide-based polyelectrolyte multilayers. *Curr. Opin. Colloid. Interface. Sci.* **2010**, *15*, 417-26. DOI

Disclaimer/Publisher's Note: All statements, opinions, and data contained in this publication are solely those of the individual author(s) and contributor(s) and do not necessarily reflect those of OAE and/or the editor(s). OAE and/or the editor(s) disclaim any responsibility for harm to persons or property resulting from the use of any ideas, methods, instructions, or products mentioned in the content.



© The Author(s) 2026. Open Access This article is licensed under a Creative Commons Attribution 4.0 International License (<https://creativecommons.org/licenses/by/4.0/>), which permits unrestricted use, sharing, adaptation, distribution and reproduction in any medium or format, for any purpose, even commercially, as long as you give appropriate credit to the original author(s) and the source, provide a link to the Creative Commons license, and indicate if changes were made.